



HAL
open science

The Greenhouse Gas Budget of Southeast Asia for 2000–2019 and Pathways Toward Climate Neutrality

Masayuki Kondo, Prabir K Patra, Josep G Canadell, Philippe Ciais, Richard A Houghton, Akihiko Ito, Chandra S Deshmukh, Tomo’Omi Kumagai, Xiangzhong Luo, Umakant Mishra, et al.

► To cite this version:

Masayuki Kondo, Prabir K Patra, Josep G Canadell, Philippe Ciais, Richard A Houghton, et al.. The Greenhouse Gas Budget of Southeast Asia for 2000–2019 and Pathways Toward Climate Neutrality. *Global Biogeochemical Cycles*, 2025, 39 (9), pp.e2024GB008256. <10.1029/2024gb008256>. <hal-05294377>

HAL Id: hal-05294377

<https://hal.science/hal-05294377v1>

Submitted on 2 Oct 2025

HAL is a multi-disciplinary open access archive for the deposit and dissemination of scientific research documents, whether they are published or not. The documents may come from teaching and research institutions in France or abroad, or from public or private research centers.

L’archive ouverte pluridisciplinaire **HAL**, est destinée au dépôt et à la diffusion de documents scientifiques de niveau recherche, publiés ou non, émanant des établissements d’enseignement et de recherche français ou étrangers, des laboratoires publics ou privés.



HAL Authorization

Global Biogeochemical Cycles[®]

RESEARCH ARTICLE

10.1029/2024GB008256

Special Collection:

Regional Carbon Cycle
Assessment and Processes - 2

Key Points:

- The greenhouse gas (GHG) budgets (CO_2 , CH_4 and N_2O) of Southeast Asia for the 2000–2019 were assessed using top-down and bottom-up approaches
- The GHG budget was a net source to the atmosphere between $3,226 \pm 406 \text{ Tg CO}_2\text{eq yr}^{-1}$ and $3,406 \pm 573 \text{ Tg CO}_2\text{eq yr}^{-1}$
- Increased GHG emissions from deforestation and coal use during 2000–2019 are obstacles to achieving climate neutrality

Supporting Information:

Supporting Information may be found in the online version of this article.

Correspondence to:

M. Kondo,
redmk92@gmail.com

Citation:

Kondo, M., Patra, P. K., Canadell, J. G., Ciais, P., Houghton, R. A., Ito, A., et al. (2025). The greenhouse gas budget of Southeast Asia for 2000–2019 and pathways toward climate neutrality. *Global Biogeochemical Cycles*, 39, e2024GB008256. <https://doi.org/10.1029/2024GB008256>



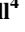


Received 3 JUN 2024

Accepted 8 SEP 2025

Author Contributions:

Conceptualization: Masayuki Kondo
Data curation: Prabir K. Patra, Richard A. Houghton, Akihiko Ito, Stephen Sitch, Ben Poulter, Hanqin Tian, Ronny Lauerwald, Judith A. Rosentreter, Naveen Chandra, Tazu Saeki, Marielle Saunois, Ingrid T. Luijkx, Takashi Maki, Takashi Nakamura
Formal analysis: Masayuki Kondo
Investigation: Masayuki Kondo
Methodology: Masayuki Kondo
Validation: Masayuki Kondo
Visualization: Masayuki Kondo, Kirari Hirabayashi
Writing – original draft: Masayuki Kondo

The Greenhouse Gas Budget of Southeast Asia for 2000–2019 and Pathways Toward Climate Neutrality

Masayuki Kondo¹ , Prabir K. Patra^{2,3} , Josep G. Canadell⁴ , Philippe Ciais⁵ , Richard A. Houghton⁶ , Akihiko Ito^{7,8} , Chandra S. Deshmukh⁹ , Tomo'omi Kumagai^{7,10,11} , Xiangzhong Luo^{12,13} , Umakant Mishra^{14,15} , Atul K. Jain¹⁶ , Wei Li¹⁷ , Gerbrand Koren¹⁸ , Stephen Sitch¹⁹ , Ben Poulter²⁰ , Hanqin Tian²¹ , Ana Bastos²² , Ronny Lauerwald²³ , Judith A. Rosentreter²⁴ , Naveen Chandra² , Tazu Saeki⁸ , Marielle Saunois⁵ , Ingrid T. Luijkx²⁵ , Takashi Maki²⁶ , Takashi Nakamura²⁷ , Kirari Hirabayashi²⁸ , Takeshi Hirano²⁹ , and Nobuko Saigusa⁸

¹The IDEC Institute - Center for Peaceful and Sustainable Futures (CEPEAS), Network for Education and Research on Peace and Sustainability (NERPS), Seto Inland Sea Carbon Neutral Research Center (S-CNC), Graduate School of Humanities and Social Sciences International Economic Development Program (IEDP), Graduate School of Innovation and Practice for Smart Society (SmaSo), Hiroshima University, Higashi-Hiroshima, Japan, ²Research Institute for Global Change, Japan Agency for Marine–Earth Science and Technology (JAMSTEC), Yokohama, Japan, ³Research Institute for Humanity and Nature (RIHN), Kyoto, Japan, ⁴Global Carbon Project, Commonwealth Scientific and Industrial Research Organisation–Environment, Canberra, ACT, Australia, ⁵Laboratoire des Sciences du Climat et de l'Environnement, LSCE/IPSL, CEA-CNRS-UVSQ, Université Paris-Saclay, Palaiseau, France, ⁶Woodwell Climate Research Center, Falmouth, MA, USA, ⁷Graduate School of Agricultural and Life Sciences, The University of Tokyo, Tokyo, Japan, ⁸Earth System Division, National Institute for Environmental Studies, Tsukuba, Japan, ⁹Asia Pacific Resources International Ltd., Pekanbaru, Indonesia, ¹⁰Institute for Space-Earth Environmental Research, Nagoya University, Nagoya, Japan, ¹¹Water Resources Research Center, University of Hawai'i at Mānoa, Honolulu, HI, USA, ¹²Department of Geography, National University of Singapore, Singapore, Singapore, ¹³Center for Nature-based Climate Solutions, Department of Biological Sciences, National University of Singapore, Singapore, Singapore, ¹⁴Computational Biology and Biophysics, Sandia National Laboratories, Livermore, CA, USA, ¹⁵Lawrence Berkeley National Laboratory, Joint BioEnergy Institute, Emeryville, CA, USA, ¹⁶Department of Climate, Meteorology and Atmospheric Sciences, University of Illinois at Urbana–Champaign, Urbana, IL, USA, ¹⁷Department of Earth System Science, Ministry of Education Key Laboratory for Earth System Modeling, Institute for Global Change Studies, Tsinghua University, Beijing, China, ¹⁸Copernicus Institute of Sustainable Development, Utrecht University, Utrecht, The Netherlands, ¹⁹Faculty of Environment, Science and Economy, University of Exeter, Exeter, UK, ²⁰Spark Climate Solutions, San Francisco, CA, USA, ²¹Department of Earth and Environmental Sciences, Center for Earth System Science and Global Sustainability, Schiller Institute for Integrated Science and Society, Boston College, Chestnut Hill, MA, USA, ²²Department of Biogeochemical Integration, Max Planck Institute for Biogeochemistry, Jena, Germany, ²³Université Paris-Saclay, INRAE, AgroParisTech, UMR ECOSYS, Palaiseau, France, ²⁴Faculty of Science and Engineering, Southern Cross University, Lismore, NSW, Australia, ²⁵Meteorology and Air Quality Department, Wageningen University and Research, Wageningen, The Netherlands, ²⁶Meteorological Research Institute, Tsukuba, Japan, ²⁷Japan Meteorological Agency, Tokyo, Japan, ²⁸Seto Inland Sea Carbon Neutral Research Center (S-CNC), Hiroshima University, Higashi-Hiroshima, Japan, ²⁹Research Faculty of Agriculture, Hokkaido University, Sapporo, Japan

Abstract Member countries of the Association of Southeast Asian Nations ratified the Paris Agreement and have initiated their own efforts to reduce greenhouse gas (GHG) emissions. However, the progress of these countries toward climate neutrality remains uncertain. Here, we estimated the combined budget for carbon dioxide (CO_2), methane (CH_4), and nitrous oxide (N_2O) in Southeast Asia for 2000–2019 using bottom-up and top-down approaches. The CO_2 emissions from deforestation were the largest source, followed by anthropogenic fire emissions, which together exceeded the CO_2 uptake by natural vegetation and land-use change legacy (e.g., regrowth), yielding a net source of CO_2 in the biosphere. The region's biosphere was also a net source of CH_4 and N_2O , which, combined with the CO_2 budget, makes the Southeast Asian biosphere a net source of GHGs to the atmosphere, ranging from $2,003.2 \pm 406.1 \text{ Tg CO}_2\text{eq yr}^{-1}$ (bottom-up) to $2,227.5 \pm 572.8 \text{ Tg CO}_2\text{eq yr}^{-1}$ (top-down) for 2000–2019. Among non-biospheric GHG emissions (e.g., fossil fuels and waste-related emissions), coal usage has resulted in an unprecedented increase in CO_2 emissions. The total GHG budget (the biospheric GHG budget plus the non-biospheric GHG fluxes) was calculated as a net source of $3,226.3 \pm 406.2 \text{ Tg CO}_2\text{eq yr}^{-1}$ (bottom-up) and $3,406.4 \pm 572.9 \text{ Tg CO}_2\text{eq yr}^{-1}$ (top-down) for 2000–2019. Our study revealed that Southeast Asia is experiencing the dual challenge of large emissions from

Writing – review & editing:

Masayuki Kondo, Prabir K. Patra, Josep G. Canadell, Philippe Ciais, Richard A. Houghton, Akihiko Ito, Chandra S. Deshmukh, Tomo'omi Kumagai, Xiangzhong Luo, Umakant Mishra, Atul K. Jain, Wei Li, Gerbrand Koren, Stephen Sitch, Ana Bastos, Ronny Lauerwald, Judith A. Rosentreter, Naveen Chandra, Tazu Saeki, Kirari Hirabayashi, Takeshi Hirano, Nobuko Saigusa

deforestation and coal usage, necessitating the implementation of urgent mitigation strategies to ensure climate neutrality.

Plain Language Summary Southeast Asia is characterized by intense human activities that contribute to increased greenhouse gas (GHG) emissions. To meet the Paris Agreement goals, member countries of the Association of Southeast Asian Nations need to suppress active land-use changes and fossil-fuel usage without compromising economic growth. However, whether a region's GHG budget acts as a net sink or source and the possibility of achieving climate neutrality in the region remain uncertain. Our study is the first to estimate a comprehensive GHG budget for Southeast Asia, encompassing all major natural and anthropogenic sources and sinks of the three major GHGs (CO₂, CH₄, and N₂O) for 2000–2019. The results revealed that the GHG budget in the region was a net source to the atmosphere, with the estimates ranging from $3,226.3 \pm 406.2$ Tg CO₂eq yr⁻¹ to $3,406.4 \pm 572.9$ Tg CO₂eq yr⁻¹. Land-use changes in forests were a major cause of GHG emissions, followed by fire emissions. GHG emissions from coal usage rapidly increased between the 2000s and the 2010s at a rate that Southeast Asia had never experienced. To achieve climate neutrality, Southeast Asia must develop effective mitigation strategies to manage GHG emissions from land-use changes and coal usage.

1. Introduction

Southeast Asia is a complex geographic region comprising mainland and insular regions dominated by tropical forests, croplands, and savannah woodlands. The forest cover in Southeast Asia constitutes 236 million hectares (Mha), accounting for approximately 15% of the world's tropical forests (Stibig et al., 2014). Renowned as a biodiversity hotspot, the region harbors numerous endemic species; in particular, it hosts the most diverse mangrove species globally (Myers et al., 2000; Richards & Friess, 2015; Sodhi et al., 2004, 2010). The region is also home to extensive tropical peatlands covering an area of 25 Mha (with an estimated carbon pool of 69 Pg C) (Page et al., 2002).

Despite its rich ecosystems, Southeast Asia is one of the regions in the world with the highest rates of deforestation due to land use, land cover change, and forestry (LULUCF), especially the conversion of primary forests to plantations (Achard et al., 2014; Baccini et al., 2017; Mitchard, 2018; Vancutsem et al., 2021; Zeng et al., 2018). Since the early 1980s, due to government policies, the region has experienced rapid major LULUCF changes, such as the opening of large forest areas for transmigration programs in the 1990s and extensive commercial palm oil and rubber production during the 2000s (Murdiyarso et al., 2010; Xu et al., 2022). In recent decades, peat swamp forests have experienced rapid decline due to the expansion of plantations (Carlson et al., 2012, 2018; Hooijer et al., 2012; Miettinen et al., 2016; Page et al., 2002; Wijedasa et al., 2018). In addition, the climate of Southeast Asia is highly susceptible to El Niño–Southern Oscillation (ENSO) (Cai et al., 2019). Notably, synergies between rapid deforestation and ENSO-driven droughts have triggered several extreme episodes of GHG emissions into the atmosphere during fire events in Southeast Asia (Field et al., 2009; Page et al., 2002; van der Werf et al., 2008).

The Association of Southeast Asian Nations (ASEAN) member states ratified the Paris Agreement and initiated their own efforts to reduce greenhouse gas (GHG) emissions. Factors that exacerbate GHG emissions in the region, such as LULUCF activities, ENSO-induced droughts, and continued economic development in the region, must be managed to bring the region's emissions trajectory in line with scenarios stabilizing the climate at 1.5°C or well-below 2°C (Qiu et al., 2024). However, due to the lack of a scientific and integrated assessment of these GHG emissions, the prospects of exceeding the Paris Agreement and achieving climate neutrality (net zero GHG emissions by balancing emissions to be less than or equal to those removed) in Southeast Asia remain highly uncertain.

To support the development of climate neutrality pathways in Southeast Asia, the current state of the region's GHG budget and its evolution in recent decades must be understood. In the current policy environment, wherein such an understanding is sought globally, the second phase of REgional Carbon Cycle Assessment and Processes (RECCAP2), an international initiative of the Global Carbon Project, was implemented to assess the regional GHG budgets of land and ocean (Poulter et al., 2022). To guide this process, RECCAP2 has established a robust

framework for regional GHG budget assessments (Ciais et al., 2022). In Southeast Asia, compared to when the carbon dioxide (CO₂) budget was assessed for the first time (Kondo, Ichii, Patra, Canadell, et al., 2018), new CO₂ flux data sets have become available, largely owing to the efforts of RECCAP2, which include data sets for emissions from inland water, estuaries, and coasts (Lauerwald et al., 2023; Rosentreter et al., 2023). In addition, data-driven and process-based estimates of regional methane (CH₄) and nitrous oxide (N₂O) emissions, including those from the industrial, agricultural, and livestock sectors, wetlands, and coastal regions, are widely available (Crippa et al., 2023; McDuffie et al., 2020; Rosentreter et al., 2023; Saunois et al., 2020). This leads to the realization that, for the first time in Southeast Asia, estimates of CO₂, CH₄, and N₂O budgets can be analyzed and managed to meet scientific and climate-policy needs.

As part of RECCAP2, we developed decadal budgets for CO₂, CH₄, and N₂O and combined GHG budgets in Southeast Asia for 2000–2019 with the aim of elucidating the contributions of individual components of natural and anthropogenic origins and the state of the transitions toward climate neutrality. Following the RECCAP2 protocol (Ciais et al., 2022), the GHG budget estimation conducted in this study relied on two independent approaches: top-down estimates of the net GHG flux from atmospheric inversions and bottom-up estimates that integrated the individual components of the GHG budget based on national inventory, modeling, and empirically upscaled observations. Through budget evaluation, we assessed the role of representative anthropogenic activities in the GHG budget (e.g., fossil fuel use, LULUCF, agriculture, and livestock). Furthermore, we illustrate the uncertainties in the approaches used as the basis for budget assessment, with a particular focus on the individual component fluxes that most significantly affected our assessment. Lastly, with the estimated current GHG budgets, we discuss the region's potential for achieving climate neutrality and realizing sustainable development and propose possible pathways for achieving these goals.

2. Materials and Methods

2.1. Study Region

The Southeast Asian region considered for this study comprised 12 countries, including members of the Association of Southeast Asian Nations (ASEAN), Brunei Darussalam, Cambodia, Indonesia, Laos, Malaysia, Myanmar, Singapore, Thailand, Vietnam, and the Philippines, and two non-ASEAN countries, East Timor and Papua New Guinea (PNG) (Figure 1). This definition, based on the regional partitions made for RECCAP2, differs from the United Nations Geoscheme for Southeast Asia, wherein PNG is excluded. For regional delineation, we utilized the National Identifier Grid v4.11 (URL: https://developers.google.com/earth-engine/datasets/catalog/CIESIN_GPWv411_GPW_National_Identifier_Grid).

2.2. Framework of the Greenhouse Gas (GHG) Budget Assessment

In this study, the GHG budget assessment for Southeast Asia was conducted using the bottom-up and top-down approaches outlined in the RECCAP2 protocol by Ciais et al. (2022) (see Figure 2). The bottom-up approach considered individual fluxes within land-freshwater system and emissions embedded in traded products outside the boundaries of Southeast Asia. These fluxes included emissions and sinks from fossil fuel use, waste disposal and burning, geological weathering and seepage, manure management, land vegetation processes, land-use changes in forests, agricultural and natural soil processes, peat decomposition and burning, inland water outgassing from lakes and rivers, and coastal vegetation processes (Figure 2). Additionally, the approach incorporates the lateral transport of carbon through river export and carbon trade via wood and crop products. The top-down approach used in this study was based on the outcomes of atmospheric inversions, which inversely estimated the net GHG flux using modeled atmospheric transport and atmospheric observations of GHGs. The utilization of these approaches in estimating the GHG budget and its components was leveraged based on various independent data sets to assess the robustness of our current understanding of the overall GHG balance and its attributions to independent component fluxes.

2.3. Components of the Bottom-Up CO₂ Budget

2.3.1. Fossil Fuel Emissions: F_{fossil}

Data of CO₂ emissions from fossil fuel usage were obtained from the International Energy Agency (IEA) 2023 (URL: <https://www.iea.org/>). The IEA 2023 data set encompassed emissions from three major fossil fuel types:

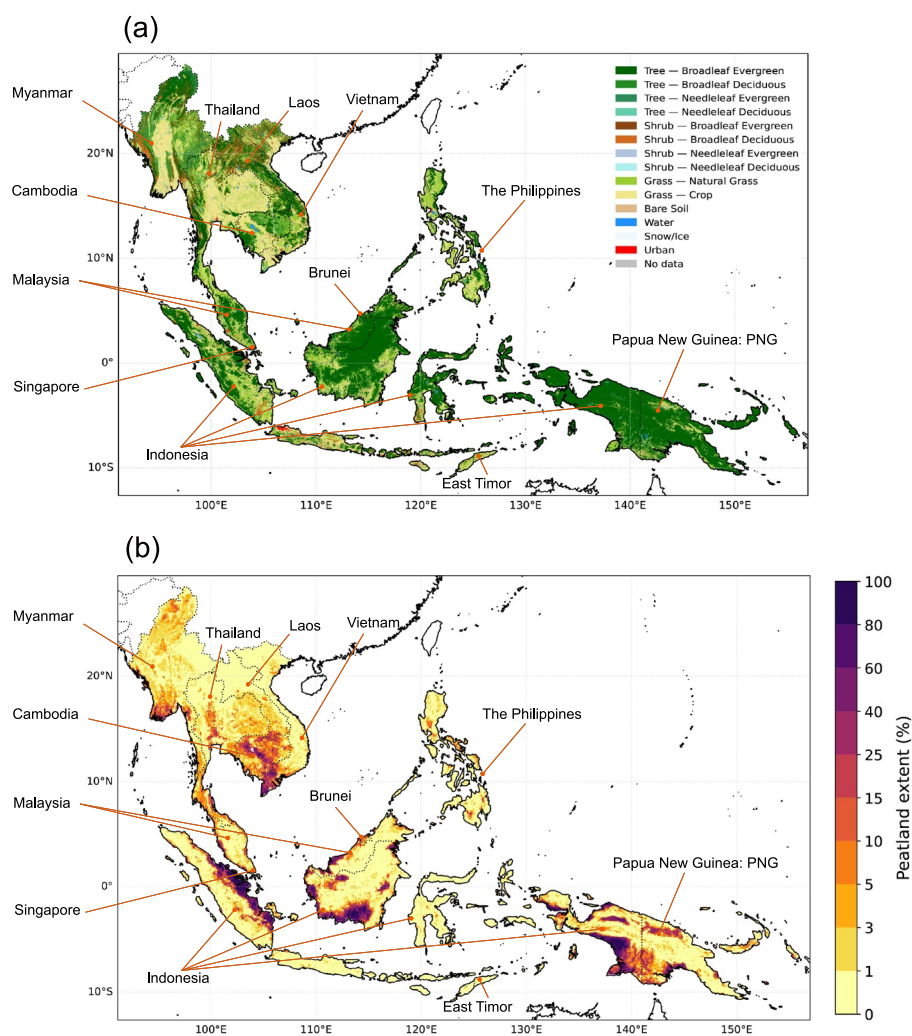


Figure 1. Geolocation of the countries and land-cover types in the Southeast Asian region considered in this study. (a) The map presenting the land cover classification obtained from the European Space Agency–Climate Change Initiative (Li et al., 2018) and (b) the peatland extent based on the global peatland extent created using machine learning (PEAT-ML) (Melton et al., 2022).

oil (crude oil, natural gas liquids, and refinery feedstocks), gas (including natural gas but excluding natural gas liquids), and coal (peat products and oil shale were incorporated in this category). The other two components, emissions from cement production and gas flaring, were obtained from independent sources, Andrew (2018) for emissions from cement production and the British Petroleum Statistical Review of World Energy (URL: <https://www.bp.com/en/global/corporate/energy-economics/statistical-review-of-world-energy.html>) for emissions from gas flaring, with both accessed from the Global Carbon Budget 2022 (Friedlingstein et al., 2022).

2.3.2. Weathering Uptake: F_{wu}

The data on CO_2 uptake by chemical weathering (F_{wu}) across Southeast Asia were obtained from a spatially explicit estimate of global weathering CO_2 uptake, based on Hartmann et al. (2009). We used the weathering CO_2 uptake model produced by Hartmann et al. (2009), which was based on an enhanced lithological classification scheme comprising a global high-resolution lithology map containing 15 lithology classes. The model was calibrated using a wide range of weathering rates per data set worldwide. According to these data, Southeast Asia is an important hotspot for weathering CO_2 uptake (Figure 2 of Hartmann et al. (2009)).

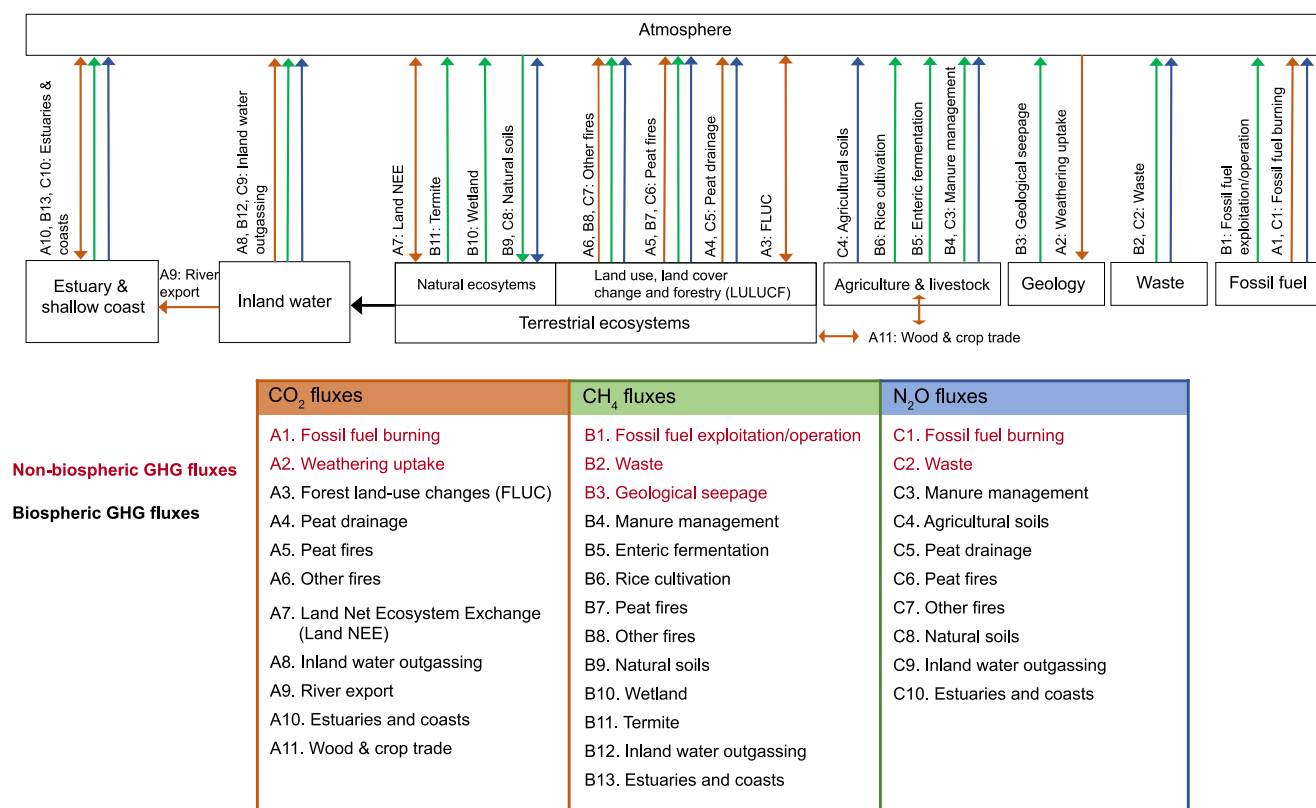


Figure 2. REgional Carbon Cycle Assessment and Processes 2 (RECCAP2) greenhouse gas (GHG) budget assessment framework for Southeast Asia. The carbon dioxide (CO₂), methane (CH₄), and nitrous oxide (N₂O) fluxes are indicated by brown, green, and blue arrows, respectively. In the bottom table, non-biospheric GHG fluxes and biospheric GHG fluxes are shown by red letters and black letters, respectively.

2.3.3. Fluxes From Land Use, Land Cover Change and Forestry (LULUCF)

CO₂ fluxes from LULUCF include CO₂ uptake and release between the terrestrial biosphere and atmosphere that result from deliberate changes in land use and land cover. In this study, we refer to the net change in CO₂ emission resulting from LULUCF as the net LULUCF flux. The net LULUCF flux was calculated by summing the following components: (a) the book-keeping estimates of the gross CO₂ emissions from deforestation and the gross of CO₂ uptake from afforestation, reforestation, and forest regrowth (hereinafter, the fluxes from land-use changes in forests will be referred to as forest land-use change (FLUC) fluxes; see Section 2.3.4); (b) emissions from decomposed peat due to drainage (Section 2.3.5); and (c) emissions from fire, including those from burning peats (Section 2.3.6).

2.3.4. Forest Land-Use Change Flux: F_{FLUC}

The forest land-use change (FLUC) flux (F_{FLUC}) was calculated based on the model employed by Houghton and Castanho (2023), which is an update of Houghton and Nassikas (2017). Hereafter, this model is referred to as the H&C model. H&C is a bookkeeping model that tracks changes in the carbon stored in living and dead vegetation (including wood products) and soil resulting from land-use changes (e.g., deforestation, wood harvesting, crop cultivation, and shifting cultivation). H&C estimated the national-level FLUC fluxes directly based on the national statistics of 5-year changes in the forest area and management stated in the Forest Resources Assessment 2020 report (FAO, 2020), and the annual changes in cropland and pasture area were derived from the Food and Agriculture Organization Corporate Statistical Database (FAOSTAT) (<http://www.fao.org/faostat/en/#data>). This study evaluated the H&C estimates of the net FLUC flux, gross FLUC emissions and FLUC uptake.

Dynamic global vegetation models and spatially explicit book-keeping models (such as BLUE) (Hansis et al., 2015) are used to estimate FLUC fluxes. However, for Southeast Asia, the inter-decadal variations in their estimates were previously found opposite to those calculated by Houghton and Nassikas (2017) and forest-area

estimates based on national statistics and satellite observations (Kondo et al., 2022). As described by Kondo et al. (2022), the cause of this discrepancy may be the unrealistic period of peak primary forest loss in Southeast Asia prescribed in the LULUCF forcing data (LUH2 data set) (Chini et al., 2021) used to run these models. Under such circumstances, the N&C model that directly reflects the national statistical data would be the most reliable model to provide FLUC flux estimates for Southeast Asia.

2.3.5. Emissions From Peat Decomposition Due To Drainage: $F_{\text{peat_deco}}$

Drained peatlands present a specific case of CO₂ emissions caused by LULUCF, which is dominated by the loss of soil carbon stock due to the decomposition of dry peat (rather than biomass). CO₂ emissions from peat decomposition due to drainage ($F_{\text{peat_deco}}$) were estimated using two independent data sets. One data set was acquired from Hooijer et al. (2010), who calculated the emissions based on the peatland extents of Sumatra, Kalimantan, and PNG (Wetlands International, 2003, 2004) and the unit area emission factors (EFs) related to peat depths. The other data were acquired from FAOSTAT, and the emissions were calculated using the Tier 1 method of the Intergovernmental Panel on Climate Change (IPCC) Guidelines for National Greenhouse Gas Inventories (IPCC, 2006, 2014), based on the national statistics of the organic soils drained for agriculture and the distribution of histosols.

2.3.6. Fire Emissions From Peat and Other Sources: $F_{\text{peat_fire}}$ and $F_{\text{other_fire}}$

In Southeast Asia, CO₂ emissions from fires ($F_{\text{peat_fire}}$ and $F_{\text{other_fire}}$) are not of natural origin but anthropogenic; therefore, in this study, we considered this flux as part of the LULUCF flux. The fire emission data were obtained from the Global Fire Emissions Database version 4.1s (GFED4.1s) (van der Werf et al., 2017). GFED4.1s presents an estimation of fire emissions by converting the spatial information regarding fire occurrence, specifically the Moderate Resolution Imaging Spectroradiometer (MODIS) MCD64A1 burnt area (Giglio et al., 2018), into emissions based on the EF, vegetation type, and other ancillary data. GFED4.1s provided the components of fire CO₂ emissions pertaining to grassland, shrubland, and peat fires, which are the dominant fire types in Southeast Asia.

In addition to the GFED4.1s, data pertaining to fire emissions from organic soil in Southeast Asian countries were obtained from FAOSTAT. FAOSTAT provided national-scale fire emission data using the annual burned area data derived from MODIS MCD64A1 (Giglio et al., 2018) and the EFs of peatland fires acquired from the IPCC Wetlands Supplement (IPCC, 2014). Note that the FAOSTAT's "fire emissions from organic soil" data set for Southeast Asia assumed that the emissions were from peat burning.

2.3.7. Natural Ecosystem Carbon Flux: $F_{\text{nat_veg}}$

The carbon flux in natural ecosystems ($F_{\text{nat_veg}}$) in this study is specifically the net ecosystem exchange (NEE). We estimated land NEE in Southeast Asia using an ensemble of 16 Dynamic global vegetation model simulations from the historical carbon cycle model intercomparison project version 10 (TRENDY v10) (Friedlingstein et al., 2022). The TRENDY model simulations spanned the period from the pre-industrial equilibrium (assumed to be at the beginning of the 1700s) to 2020; the simulations were conducted using observation-based forcing data of atmospheric CO₂ and climate. Among the several types of TRENDY v10 simulations, we used the results of simulation S2, which considered variations in CO₂ concentrations and climate. Note that S2 does not consider LULUCF.

2.3.8. River Export Flux: F_{export}

The lateral river transport of carbon to the Southeast Asian coast (F_{export}) was estimated at the river basin scale using the Global Nutrient Export from WaterSheds (NEWS) model framework (Mayorga et al., 2010). The modeled loads of dissolved organic carbon (DOC), dissolved inorganic carbon (DIC), and particulate organic carbon (POC) applied in this study, based on Mayorga et al. (2010) and Hartmann et al. (2009) (for details, refer to Zscheischler et al., 2017), were generated using drivers corresponding to the year 2000, which included the observed hydroclimatological forcing data. Some parameters and observed loads were based on the data from the previous two decades. The adjusted grid-cell-scale exports were aggregated to the basin scale using the NEWS basin definitions (Mayorga et al., 2010) and then reduced by applying the NEWS-based basin-scale consumption water-removal factor acquired from the data on irrigation withdrawals (Mayorga et al., 2010). This study

considered carbon export from rivers as a part of the CO₂ sink, as it was originally a CO₂ sink from the atmosphere into vegetation and ultimately into soils, which is then leached into rivers and transported to the ocean rather than going directly to the atmosphere. This flux has a mixed origin from both natural and anthropogenic sources, which we are unable to partition in this study.

2.3.9. Inland Water Outgassing Flux: $F_{\text{outgassing}}$

The river and lake CO₂ outgassing flux ($F_{\text{outgassing}}$) data for Southeast Asia were obtained from previous studies compiled by Lauerwald et al. (2023). The metadata contain published values of CO₂ outgassing from lakes and rivers worldwide, which were then broken down into the RECCAP2 land regions. The fluxes were rescaled to consistent estimates of the surface area of lakes, reservoirs (HydroLAKES; Messenger et al., 2016) and rivers (Allen & Pavelsky, 2018). For the entire Southeast Asian region, the metadata provided four, five, eight, and five values for CO₂ outgassing from rivers, natural lakes, reservoir lakes, and lakes regulated by dams, respectively.

The four estimates of CO₂ outgassing from rivers varied widely from 161.6 Tg CO₂ yr⁻¹ to 2,968.8 Tg CO₂ yr⁻¹; thus, the choice of the representative value (maximum, minimum, median, and average) largely affected the CO₂ budget. The total basin area of the five major river systems in Southeast Asia (the Irrawaddy, Salween, Mekong, Chao Phraya, and Red Rivers) is approximately 1,333,800 km², accounting to 16% of the total basin area of the major river system in South America. However, the four estimates of the data set indicated that the maximum estimate of the CO₂ outgassing from rivers in Southeast Asia was as high as 88% of that in South America, followed by 44%, 40%, and 28%. The fact that the rate of CO₂ outgassing from rivers in Southeast Asia is higher than that in South America is not supported by evidence, and a previous study, on which the maximum estimate is based, suggests that the estimate for Southeast Asia may be overestimated because the CO₂ data calculated from the region's pH, alkalinity, and temperature were biased toward high values (Raymond et al., 2013). Therefore, we used the lowest value of the four available estimates for the budget assessment. The mean values were used for the other outgassing estimates (i.e., natural lakes, reservoir lakes, and lakes regulated by dams), as their values did not vary significantly.

2.3.10. Estuarine and Coastal Vegetation Flux: $F_{\text{est_coast}}$

In addition to land CO₂ fluxes, we considered coastal CO₂ fluxes, such as the water-air CO₂ fluxes in estuaries and NEE in coastal wetland ecosystems ($F_{\text{est_coast}}$) (Rosentreter et al., 2023). The data-driven meta-analysis presented by Rosentreter et al. (2023) contains information on three types of estuaries: tidal systems and deltas, lagoons, and fjords (not relevant to Southeast Asia), along with three types of coastal vegetation: mangroves, salt marshes, and seagrass, with the surface area estimated for each coastal type globally. In the coastal meta-analysis, the water-air or NEE flux rates compiled from the literature were averaged over space and time based on the data from each site. The estimated areal flux rates were then grouped for each RECCAP2 region and for each estuary and coastal vegetation type. Finally, non-parametric bootstrapping was performed on the flux rates and the results were scaled to the surface area of each coastal ecosystem type in each RECCAP2 region. Further information on coastal CO₂ flux estimation can be found in Rosentreter et al. (2023). The regional coastal CO₂ flux estimates for Southeast Asia were based on 20 sites for tidal system and delta fluxes and five sites for mangrove NEE; for other coastal ecosystems where less data were available, the global statistics aggregated for the RECCAP2 regions were used (Rosentreter et al., 2023).

2.3.11. Wood and Crop Trade Flux: F_{trade}

We estimated the carbon associated with the export and import of wood and crop products in Southeast Asia (F_{trade}), using the method described by Ciais et al. (2022). Country-based economic data on trade volume and carbon content were obtained from the FAOSTAT for individual wood and crop products. The gross amounts of imported and exported carbon for individual products were estimated using trade volume and carbon content. The total net trade flux for crops and wood was calculated based on the difference between exported and imported carbon estimated in this study. As for river carbon exports, we considered the carbon fluxes resulting in wood and crop trades as part of the CO₂ sink because carbon was exported to or imported from other terrestrial regions, rather than going directly into the atmosphere.

2.4. Components of the Bottom-Up CH₄ and N₂O Budgets

2.4.1. Emissions From Fossil Fuels and Waste: F_{fossil} and F_{waste} (CH₄ and N₂O)

In this study, the direct anthropogenic emissions of CH₄ and N₂O were the combustion or exploitation of fossil fuels (F_{fossil}) and waste disposal, burning, and wastewater treatment (F_{waste}). Similar to CO₂, CH₄ and N₂O emissions from fossil fuel burning and exploitation in Southeast Asia (F_{fossil}) were primarily sourced from the IEA 2023 data set, including emissions from oil and gaseous fuels as well as emissions from coal mining. For emissions from waste, we employed an ensemble of two global emission inventories: the Community Emissions Data System (CEDS v2021) (McDuffie et al., 2020) and Emissions Database for Global Atmospheric Research (EDGARv7.0) (Crippa et al., 2023).

2.4.2. Geological Seepage Flux: F_{gs} (CH₄)

The data on CH₄ emissions from geological seepage, F_{gs} (the natural degassing of hydrocarbons from the Earth's crust) were obtained from the global gridded data set presented by Etiope et al. (2019). The data set provides information on four types of global seepages: (a) onshore hydrocarbon macro-seeps, including mud volcanoes, (b) submarine (offshore) seeps, (c) diffused micro-seepage, and (d) geothermal manifestations. We extracted these data for Southeast Asia and used a combined value for the CH₄ budget assessment.

2.4.3. Emissions From Livestock and Agriculture: F_{manure} , F_{enteric} , and F_{rice} (CH₄), and F_{manure} and F_{agrisoil} (N₂O)

Livestock and agriculture are crucial anthropogenic sources of CH₄ and N₂O emissions. The data for these emissions were derived from an ensemble of three global emission inventories: FAOSTAT, CEDS v2021, and EDGARv7.0. Each inventory encompassed emissions from the common livestock and agricultural sectors necessary for CH₄ and N₂O budget assessments. From these data sets, we estimated CH₄ emissions from manure management (F_{manure}), enteric fermentation (F_{enteric}), and rice cultivation (F_{rice}), as well as N₂O emissions from manure management (F_{manure}) and agricultural soils (F_{agrisoil}).

2.4.4. Emissions From Peat Decomposition Due To Drainage: $F_{\text{peat_deco}}$ (N₂O)

The N₂O emissions from peat decomposition due to drainage ($F_{\text{peat_deco}}$) estimated in this study were based on FAOSTAT (described in Section 2.3.5), which represents the only available estimate.

2.4.5. Fire Emissions: $F_{\text{peat_fire}}$ and $F_{\text{other_fire}}$ (CH₄ and N₂O)

CH₄ and N₂O emissions from fires encompassing peat burning ($F_{\text{peat_fire}}$) and other types of burning ($F_{\text{other_fire}}$) were obtained from GFED4.1s. As with CO₂, the CH₄ emissions from peat burning were acquired from FAOSTAT, termed “fire emissions from organic soil.” FAOSTAT data for emissions from peat burning were not available for N₂O.

2.4.6. Emissions From Wetlands: F_{wet} (CH₄)

CH₄ emissions from wetlands (F_{wet}) were estimated using an ensemble of 13 process-based model simulations previously prepared for the Global Methane Budget (Saunois et al., 2020). These models calculated CH₄ emissions as the product of the emission flux density and methane-producing surface extent. All models were forced by common data sets, such as the reconstructed climate fields (CRU-JRA) and the remote sensing-based dynamical wetland area data set (Wetland Area Dynamics for Methane Modeling: WAD2M).

2.4.7. Oxidative Consumption by and Emissions From Natural Soils: F_{soil} (CH₄ and N₂O)

A process-based model simulation from Vegetation Integrated Simulator for Trace gases (VISIT) (Ito et al., 2023) was used to quantify the oxidative consumption of atmospheric CH₄ by natural soils (F_{soil}). VISIT calculates CH₄ transfer from the atmosphere to the soil base using a semi-empirical scheme (Curry, 2007) embedded within the model, which parameterizes soil airspace gas diffusivity using an empirical equation for soil temperature and moisture content. Microbial oxidation activity was also calculated using the simulated soil temperature and moisture content. Following Curry (2007), VISIT assumes that the cropland fraction affects the soil oxidation rate, while considering the effect of nitrogen fertilizers on the reduction of CH₄ oxidation rates.

N_2O emissions from natural soils (F_{soil}) were obtained from seven process-based model simulations of the Global N_2O Model Intercomparison Project (NMIP) (Tian et al., 2018, 2020). From the seven available simulations (S0–S6), we used S2, which considers the spatiotemporal effects of climate, atmospheric CO_2 , LULUCF, nitrogen deposition, and fertilizer. However, this simulation did not consider the effects of manure management.

2.4.8. Emissions From Termite Activity: $F_{termite}$ (CH_4)

CH_4 emissions from termite activity ($F_{termite}$) were obtained from process-based model simulations conducted using VISIT (Ito, 2023). The simulation of CH_4 emissions was based on prescribed global data sets of field-observed termite colonies, calculated as the product of termite biomass density and EFs. Termite biomass was estimated using a regression model that represented the dependence on gross primary productivity.

2.4.9. Inland Water Outgassing: $F_{outgassing}$ (CH_4 and N_2O)

Similar to CO_2 , the data for river and lake CH_4 and N_2O outgassing ($F_{outgassing}$) in Southeast Asia were obtained from the data sets compiled by Lauerwald et al. (2023).

2.4.10. Estuarine and Coastal Vegetation Fluxes: F_{est_coast} (CH_4 and N_2O)

Data for CH_4 and N_2O fluxes from estuarine and coastal vegetation (F_{est_coast}) in Southeast Asia were obtained from a meta-analysis by Rosentreter et al. (2023). In Southeast Asia, the analysis included 11 sites for tidal systems and delta CH_4 fluxes and 11 sites for mangrove CH_4 fluxes. The available N_2O data for Southeast Asia include eight tidal systems and delta sites. All other coastal ecosystem GHG fluxes in Southeast Asia were estimated based on global statistics (Rosentreter et al., 2023).

2.5. Top-Down Approach

Atmospheric inversions or top-down analyses provide estimates of the net CO_2 flux at the surface resulting from all fluxes between the biosphere and atmosphere. In this study, we estimated the net CO_2 flux using nine atmospheric inverse frameworks: ACTM_CONTRAIL (Saeki & Patra, 2017), CAMS (Chevallier et al., 2010), Carbon-Tracker CT2022 (Peters et al., 2007), Carbon-Tracker-Europe (van der Laan-Luijckx et al., 2017), CMS-flux (Liu et al., 2021), JMA2021 (Maki et al., 2023), GOSAT L4A (Maksyutov et al., 2013), MIROC4-ACTM (Chandra et al., 2022), and UoE (Feng et al., 2016). In situ surface observations of atmospheric CO_2 over Southeast Asia are limited, and most atmospheric inversions have been carried out without constraints provided by direct CO_2 measurements in the region. Therefore, the magnitude and trend of the net CO_2 flux in the region depend on the performance of the constraints in the nearby regions. Two models (ACTM_CONTRAIL and JMA2021) used CO_2 observations from the upper troposphere obtained by Japan Airlines (JAL) at cruising altitudes between Tokyo and Sydney/Brisbane (Comprehensive Observation Network for TRace gases by AirLiner: CONTRAIL, Matsueda et al., 2008; Machida et al., 2008). One model (GOSAT L4A) uses column-averaged CO_2 observations acquired by the GOSAT satellite (Yoshida et al., 2013) as a constraint.

The net CH_4 flux was based on ten CH_4 inversion systems obtained from the Global Methane Budget (Saunois et al., 2020). These inversions were based on tower CH_4 observations and/or column-averaged CH_4 observations acquired by the GOSAT satellite. The inversion models used in this study were Carbon-Tracker-Europe (Tsuruta et al., 2017), GELCA (Ishizawa et al., 2016), LMDz-PYVAR (Zheng, Chevallier, Ciais, Yin, & Wang, 2018; Zheng, Chevallier, Ciais, Yin, Deeter et al., 2018), MIROC4-ACTM (Chandra et al., 2021; Patra et al., 2016, 2018), NICAM-TM (Niwa, Tomita, et al., 2017; Niwa, Fujii, et al., 2017), NIES-TM, NIES-TM-FLEXPART (Maksyutov et al., 2021; Wang et al., 2019), TM5-CAMS (Pandey et al., 2016; Segers & Houwelling, 2018), TM5-4DVAR (Bergamaschi et al., 2013), and TOMCAT (McNorton et al., 2018).

We estimated the net N_2O flux using four independent N_2O inversion systems described by Tian et al. (2020). These models included GEOS-Chem (Wells et al., 2015), INVICAT (Wilson et al., 2014), MIROC4-ACTM (Patra et al., 2018), and PyVAR_CAMS (Thompson et al., 2014). Unlike the inversion models used for CO_2 and CH_4 inversions, none of the four N_2O inversion systems was constrained by atmospheric N_2O measurements (e.g., aircraft or satellites) over Southeast Asia. Therefore, the accuracy of top-down N_2O budgets for Southeast Asia may be limited.

2.6. Budget Assessment

In this study, we estimated two types of GHG budgets: the biospheric GHG budget (accounting for only the fluxes in and out of the biosphere) and the total GHG budget (including non-biospheric fluxes, i.e., emissions due to the extraction and use of fossil fuels, waste disposal and burning, and geological fluxes, such as chemical weathering and geological seepage). The biospheric bottom-up (BU) and top-down (TD) CO₂, CH₄, and N₂O budgets are constructed as follows:

$$\text{Biospheric BU}_{\text{CO}_2} = F_{\text{FLUC}} + F_{\text{peat_deco}} + F_{\text{peat_fire}} + F_{\text{other_fire}} + F_{\text{nat_veg}} + F_{\text{outgassing}} + F_{\text{export}} + F_{\text{est_coast}} + F_{\text{trade}} \quad (1)$$

$$\text{Biospheric BU}_{\text{CH}_4} = F_{\text{manure}} + F_{\text{enteric}} + F_{\text{rice}} + F_{\text{peat_fire}} + F_{\text{other_fire}} + F_{\text{wet}} + F_{\text{termite}} + F_{\text{outgassing}} + F_{\text{est_coast}} \quad (2)$$

$$\text{Biospheric BU}_{\text{N}_2\text{O}} = F_{\text{manure}} + F_{\text{agrisoil}} + F_{\text{peat_deco}} + F_{\text{peat_fire}} + F_{\text{other_fire}} + F_{\text{soil}} + F_{\text{outgassing}} + F_{\text{est_coast}} \quad (3)$$

The results of atmospheric inversions cannot be directly compared with bottom-up estimates due to the difference in components included in net flux estimates (Kondo et al., 2020). Therefore, lateral CO₂ fluxes, such as river carbon transport and wood and crop trade, were added to the net CO₂ flux estimated by atmospheric inversions so that both the top-down and bottom-up approaches accounted for the same fluxes in the CO₂ budgets (Ciais et al., 2022; Kondo et al., 2020). With the necessary adjustments, the biospheric top-down CO₂, CH₄, and N₂O budgets (excluding non-biospheric GHG fluxes) can be represented as follows:

$$\text{Biospheric TD}_{\text{CO}_2} = \text{CO}_2 \text{ inversion} - F_{\text{export}} - F_{\text{trade}} \quad (4)$$

$$\text{Biospheric TD}_{\text{CH}_4} = \text{CH}_4 \text{ inversion} \quad (5)$$

$$\text{Biospheric TD}_{\text{N}_2\text{O}} = \text{N}_2\text{O inversion} \quad (6)$$

Using the biospheric GHG budgets, the total GHG budgets were calculated by adding the non-biospheric components, as follows:

$$\text{Total BU}_{\text{CO}_2} = \text{Biospheric BU}_{\text{CO}_2} + F_{\text{fossil}} + F_{\text{wu}} \quad (7)$$

$$\text{Total BU}_{\text{CH}_4} = \text{Biospheric BU}_{\text{CH}_4} + F_{\text{fossil}} + F_{\text{waste}} + F_{\text{gs}} \quad (8)$$

$$\text{Total BU}_{\text{N}_2\text{O}} = \text{Biospheric BU}_{\text{N}_2\text{O}} + F_{\text{fossil}} + F_{\text{waste}} \quad (9)$$

$$\text{Total TD}_{\text{CO}_2} = \text{Biospheric TD}_{\text{CO}_2} + F_{\text{fossil}} + F_{\text{wu}} \quad (10)$$

$$\text{Total TD}_{\text{CH}_4} = \text{Biospheric TD}_{\text{CH}_4} + F_{\text{fossil}} + F_{\text{waste}} + F_{\text{gs}} \quad (11)$$

$$\text{Total TD}_{\text{N}_2\text{O}} = \text{Biospheric TD}_{\text{N}_2\text{O}} + F_{\text{fossil}} + F_{\text{waste}} \quad (12)$$

Finally, the total impact of the three GHGs on global warming (in terms of CO₂ equivalent: CO₂eq) was calculated for the bottom-up and top-down approaches using the global warming potentials over a 100-year time horizon (GWP100). Following the guidelines in IPCC AR6 (Canadell et al., 2021; Forster et al., 2021), we used a GWP100 value of 27.0 for non-fossil fuel CH₄ budget components, such as the emissions of biogenetic origin (GWP_{CH₄-NFF}), 29.8 for fossil fuel fugitive CH₄ emissions (GWP_{CH₄-FF}), and 273 for the N₂O budget (GWP_{N₂O}). The integrated GHG budgets for the three gases are calculated as follows:

$$\text{GHG budget} = [\text{CO}_2] + [\text{CH}_4 - \text{fossil fuel}] \times [\text{GWP}_{\text{CH}_4-\text{FF}}] + [\text{CH}_4 - \text{non fossil fuel}] \times [\text{GWP}_{\text{CH}_4-\text{NFF}}] + [\text{N}_2\text{O}] \times \text{GWP}_{\text{N}_2\text{O}} \quad (13)$$

Table 1

Carbon Dioxide (CO₂) Budget and Its Components (Tg CO₂ yr⁻¹) for Southeast Asia in the 2000s (2000–2009), the 2010s (2010–2019), and 2000–2019

Category	Components	2000s	2010s	2000–2019
Direct human emissions	Oil, gas, and coal	815.1	1,208.4	1,011.7
	Cement production	62.2	103.0	82.6
	Gas flaring	11.9	13.1	12.5
Geology	Weathering uptake	-124.7	-124.7	-124.7
LULUCF fluxes	Gross FLUC emissions	1,824.9	2,078.4	1,951.7
	Gross FLUC uptake	-1,086.4	-1,143.7	-1,115.0
	Peat decomposition due to drainage	268.0	302.8	285.4
	Peat burning	178.0 ± 45.5	176.0 ± 51.1	192.6 ± 48.3
	Biomass burning excluding peat burning	775.8	648.8	712.3
Natural land fluxes	Vegetation carbon flux (land NEE)	-1,210.4 ± 277.9	-1,175.5 ± 300.0	-1,193.0 ± 288.9
Inland water fluxes	River export: DOC	-88.0	-88.0	-88.0
	River export: DIC	-183.3	-183.3	-183.3
	River export: POC	-113.7	-113.7	-113.7
	Outgassing from lakes and rivers	177.5	177.5	177.5
Estuarine fluxes	Tidal system, deltas, and lagoons	11.9	11.9	11.9
Coastal vegetation fluxes	Mangrove, salt marsh, and seagrasses	-178.7	-178.7	-178.7
Trade	Woods and crop	-122.0	-151.9	-137.0
Budget	Type	2000s	2010s	2000–2019
Biospheric CO ₂ budget	Bottom-up	253.6 ± 281.6	360.7 ± 304.3	308.1 ± 292.9
	Top-down	539.5 ± 344.6	683.2 ± 690.4	611.3 ± 517.5
Total CO ₂ budget	Bottom-up	1,018.0 ± 281.6	1,560.5 ± 304.3	1,289.3 ± 292.9
	Top-down	1,303.9 ± 344.6	1,883.0 ± 690.4	1,593.5 ± 517.5

Note. Land use, land cover change and forestry (LULUCF); Forest land-use changes (FLUC); Net ecosystem exchange (NEE); Dissolved organic carbon (DOC); Dissolved inorganic carbon (DIC); Particulate organic carbon (POC).

2.7. Uncertainty

The uncertainty of the GHG budget could not be precisely defined because of the absence of the physical uncertainty associated with each component flux. We could only estimate statistical uncertainty; achieving highly accurate uncertainty estimations was challenging due to the limited data availability for the region. In cases where multiple estimates were accessible for a component flux, a standard deviation of 1σ was considered after thoroughly scrutinizing the estimates. However, the majority of the component fluxes lacked sufficient multiple estimates to derive a statistically meaningful spread, often providing only one estimate. Therefore, in this budget assessment, we estimated the uncertainty of the GHG budget using the error propagation method while considering the standard deviations of 1σ from the component fluxes with more than two independent estimates

(i.e., $\delta\text{GHG} = \sqrt{(\delta\text{comp1})^2 + (\delta\text{comp2})^2 + (\delta\text{comp3})^2 \dots}$, where δGHG is the uncertainty of the CO₂ budget, and δcomp is the 1σ standard deviation for a component flux).

3. Greenhouse Gas (GHG) Budget of Southeast Asia

3.1. CO₂ Budget

Table 1 presents the components of the CO₂ budget for the 2000s, the 2010s, and 2000–2019. The land NEE (CO₂ exchange in natural ecosystems) showed the largest CO₂ sink, amounting to -1,193.0 ± 288.9 Tg CO₂ yr⁻¹ for 2000–2019, closely followed by the gross FLUC uptake (i.e., CO₂ uptake from reforestation and regrowth: at -1,115.0 Tg CO₂ yr⁻¹). These two components contributed to 40% and 37% of the total gross biospheric CO₂ uptake in Southeast Asia, respectively. Lateral carbon fluxes, such as river exports and wood and crop trade,

constitute 18% of gross CO₂ uptake, indicating a large amount of carbon transport to the coasts of Southeast Asia and to the ocean. Coastal ecosystems, including mangrove forests, represent the smallest proportion at 6% of the total gross biospheric CO₂ uptake.

Over the two decades, the gross FLUC emissions (i.e., emissions directly resulting from deforestation, degradation, and wood harvesting) was the most significant emission component, amounting to 1,951.7 Tg CO₂ yr⁻¹ (Table 1). This accounts for 59% of the total gross CO₂ emissions from the biosphere, followed by fire emissions (27%), in which peat fires account for 5%, and the other types of fires account for 22%. The remaining components accounted for smaller proportions, for example, emissions from peat decomposition (11%) and inland water outgassing (7%). Although Southeast Asia is home to peatlands, peat-related CO₂ emissions (peat decomposition and peat burning) comprise 24% of the gross FLUC emissions, signifying the greater impact of deforestation in the region. The gross FLUC emissions surpassed the gross FLUC uptake, resulting in a net CO₂ source (from FLUC) of 836.6 Tg CO₂ yr⁻¹. Consequently, the LULUCF flux (the sum of the gross FLUC emissions and uptake, peat drainage, peat fires, and other types of fires) in Southeast Asia collectively represented large net sources of CO₂, amounting to 2,011.3 Tg CO₂ yr⁻¹.

The biospheric CO₂ budget from the bottom-up approach represented a net source of 253.6 ± 292.9 Tg CO₂ yr⁻¹ for 2000–2019 (Table 1). This budget reflects the impact of FLUC and fire emissions, canceling and exceeding the two major gross sink components (i.e., land NEE and gross FLUC uptake). Biospheric CO₂ budget estimates obtained using the top-down approach were comparable to those using the bottom-up approach, indicating a net source of 611.3 ± 517.5 Tg CO₂ yr⁻¹ (Table 1). The CO₂ budgets from both approaches increased by approximately 100 Tg CO₂ yr⁻¹ from the 2000s to the 2010s, with increasing emissions from gross FLUC emissions contributing the most among all components.

For 2000–2019, the non-biospheric CO₂ emissions were dominated by emissions from oil, gas, and coal burning (1,011.7 Tg CO₂ yr⁻¹), followed by those from cement production (82.6 Tg CO₂ yr⁻¹) and gas flaring (12.5 Tg CO₂ yr⁻¹) (Table 1). These emissions increased substantially from the 2000s to the 2010s, with a 48% increase in emissions from oil, gas, and coal, 66% in emissions from cement production, and 11% in emissions from gas flaring. The weathering CO₂ uptake was -124.7 Tg CO₂ yr⁻¹, which canceled 11% of the CO₂ emissions from fossil fuels. The sum of these fossil fuel emissions and weathering uptake amounted to 982.1 Tg CO₂ yr⁻¹ during 2000–2019. This results in the total CO₂ budget (sum of the biospheric CO₂ budget and the non-biospheric CO₂ fluxes) being a net source of 1,289.3 ± 292.9 Tg CO₂ yr⁻¹ in the bottom-up approach and 1,593.5 ± 517.5 Tg CO₂ yr⁻¹ in the top-down approach. The increase in the total CO₂ budgets from the 2000s to the 2010s (ranging from 542.48 to 579.10 Tg CO₂ yr⁻¹) was approximately five times greater than the increase in the biospheric CO₂ budgets and was driven by rising emissions from the combustion of oil, natural gas, and coal (Table 1).

3.2. CH₄ Budget

As shown in Table 2, in the 2000s and the 2010s, all components of the CH₄ budget, except for natural soils, were net sources of CH₄ to the atmosphere. Among all the components, wetland (19.1 ± 7.50 Tg CH₄ yr⁻¹) dominated the CH₄ emissions of Southeast Asia for 2000–2019, followed by rice cultivation (8.90 ± 0.21 Tg CH₄ yr⁻¹). These two components accounted for 49% and 23% of the total CH₄ emissions from the biosphere, respectively. Other components, including emissions from enteric fermentation, fires, and termites, showed roughly equivalent magnitudes, with each contributing less than 10% of the total emissions. Oxidative consumption by natural soils was solely a net sink of the atmospheric CH₄, amounting to -2.42 Tg CH₄ yr⁻¹ in 2000–2019, canceling 6% of the total CH₄ emissions from the biosphere.

The biospheric CH₄ budget from the bottom-up approach indicated a net source of 36.2 ± 7.53 Tg CH₄ yr⁻¹ in 2000–2019 (Table 2). The top-down approach yielded a relatively consistent estimate of 46.4 ± 7.60 Tg CH₄ yr⁻¹ (Table 2). The budget estimated using the two approaches showed a moderate increase between the 2000s and the 2010s (1.5 Tg CH₄ yr⁻¹ in the bottom-up approach and 5.3 Tg CH₄ yr⁻¹ in the top-down approach), reflecting that the components of CH₄ emissions from the biosphere have not undergone rapid changes during these decades. This differs from the notable increase in emissions from in the region indicated by a process-based model study reported by Ito et al. (2023).

Regarding fossil fuels, oil and gaseous fuel extraction and coal mining were the largest CH₄ emitters in 2000–2019 (2.46 Tg CH₄ yr⁻¹ and 2.22 Tg CH₄ yr⁻¹, respectively), followed by waste disposal, waste burning, and

Table 2
Methane (CH₄) Budget (and Its Components) (Tg CH₄ yr⁻¹) for Southeast Asia in the 2000s (2000–2009), the 2010s (2010–2019), and 2000–2019

Category	Components	2000s	2010s	2000–2019
Direct human emissions	Oil and gas extraction	2.38	2.53	2.46
	Coal mining	1.33	3.11	2.22
	Waste disposal, waste burning, and waste-water treatment	1.29 ± 0.34	1.78 ± 0.29	1.54 ± 0.32
Geology	Geological seepage	1.49	1.49	1.49
Agriculture/Livestock	Manure management	0.38 ± 0.28	0.47 ± 0.35	0.42 ± 0.32
	Enteric fermentation	3.11 ± 0.03	3.45 ± 0.02	3.28 ± 0.02
	Rice cultivation	8.60 ± 0.11	9.20 ± 0.30	8.90 ± 0.21
LULUCF fluxes	Peat burning	2.21 ± 0.45	2.13 ± 0.36	2.17 ± 0.40
	Biomass burning excluding peat burning	0.67	0.56	0.62
Natural land fluxes	Wetland	18.9 ± 7.43	19.3 ± 7.57	19.1 ± 7.50
	Natural soils	-2.36	-2.49	-2.42
	Termites	1.12	1.17	1.15
Inland water fluxes	Outgassing from lakes and rivers	2.90	2.90	2.90
Estuarine fluxes	Tidal system, deltas, and lagoons	0.004	0.004	0.004
Coastal vegetation fluxes	Mangrove, salt marsh, and seagrasses	0.068	0.068	0.068
Budget	Type	2000s	2010s	2000–2019
Biospheric CH ₄ budget	Bottom-up	35.6 ± 7.45	36.7 ± 7.60	36.2 ± 7.53
	Top-down	43.8 ± 7.11	49.1 ± 8.10	46.4 ± 7.60
Total CH ₄ budget	Bottom-up	42.1 ± 7.46	45.6 ± 7.60	43.9 ± 7.53
	Top-down	50.3 ± 7.12	58.0 ± 8.10	54.1 ± 7.61

Note. Land use, land cover change and forestry (LULUCF).

wastewater treatment (1.54 ± 0.32 Tg CH₄ yr⁻¹) (Table 2). Similar to CO₂ emissions from fossil fuel use, CH₄ emissions from fossil fuel extraction (particularly from coal mining) increased more than two-folds between the 2000s and the 2010s. Geological seepage yielded CH₄ emissions of 1.49 Tg CH₄ yr⁻¹, equivalent to waste-related CH₄ emissions. However, the sum of fossil fuel and geological CH₄ emissions (7.70 Tg CH₄ yr⁻¹) remained significantly smaller than the emissions from wetlands (Table 2). Consequently, the non-biospheric emissions only contributed modestly to the total CH₄ budget (sum of the biospheric CH₄ budget and non-biospheric emissions): 43.9 ± 7.53 Tg CH₄ yr⁻¹ in the bottom-up approach and 54.1 ± 7.61 Tg CH₄ yr⁻¹ in the top-down approach. The total CH₄ budgets increased between the 2000s and the 2010s, with a rate greater than the biospheric CH₄ budgets (3.6 Tg CH₄ yr⁻¹ in the bottom-up approach and 7.7 Tg CH₄ yr⁻¹ in the top-down approach), largely due to the increased emissions from coal mining (Table 2).

3.3. N₂O Budget

Table 3 outlines the components of the N₂O budget for the 2000s, the 2010s, and 2000–2019. Among all components, emissions from natural soils were the largest (1.93 ± 0.68 Tg N₂O yr⁻¹ for 2000–2019), constituting a dominant proportion (73%) of the total N₂O emissions from the biosphere. This was followed by the agricultural soils (12%), with the remaining components contributing smaller proportions. Although emissions were relatively small, manure management, agricultural soils, and peat decomposition showed a 12%–21% increase in N₂O emissions from the 2000s to the 2010s.

The biospheric N₂O budget from the bottom-up approach indicated a net source of 2.64 ± 0.71 Tg N₂O yr⁻¹ in 2000–2019 (Table 3). The top-down approach estimates were approximately half of the bottom-up estimates, at 1.33 ± 0.49 Tg N₂O yr⁻¹. Despite a common increase in budget estimates between the 2000s and the 2010s, the bottom-up estimate showed a small increase (~5%), whereas the top-down approach showed an increase four times larger (~20%).

Table 3

Nitrous Oxide (N₂O) Budget (and Its Components) (Tg N₂O yr⁻¹) for Southeast Asia in the 2000s (2000–2009), the 2010s (2010–2019), and 2000–2019

Category	Components	2000s	2010s	2000–2019
Direct human emissions	Oil and gas	0.020	0.032	0.026
	Waste disposal, waste burning, and waste-water treatment	0.041 ± 0.028	0.053 ± 0.036	0.047 ± 0.032
Agriculture/Livestock	Manure management	0.13 ± 0.14	0.14 ± 0.15	0.13 ± 0.15
	Agricultural soils	0.30 ± 0.18	0.36 ± 0.23	0.33 ± 0.20
LULUCF fluxes	Peat decomposition due to drainage	0.17	0.19	0.18
	Peat burning	0.18	0.18	0.18
	Biomass burning excluding peat burning	0.029	0.024	0.026
Natural land fluxes	Natural soils	1.92 ± 0.66	1.94 ± 0.67	1.93 ± 0.68
Inland water fluxes	Outgassing from lakes and rivers	0.015	0.015	0.015
Estuarine fluxes	Tidal system, deltas, and lagoons	0.005	0.005	0.005
Coastal vegetation fluxes	Mangrove, salt marsh, and seagrasses	0.002	0.002	0.002
Budget	Type	2000s	2010s	2000–2019
Biospheric N ₂ O budget	Bottom-up	2.58 ± 0.70	2.70 ± 0.73	2.64 ± 0.71
	Top-down	1.21 ± 0.41	1.45 ± 0.57	1.33 ± 0.49
Total N ₂ O budget	Bottom-up	2.64 ± 0.70	2.78 ± 0.73	2.71 ± 0.71
	Top-down	1.41 ± 0.41	1.67 ± 0.57	1.54 ± 0.49

Note. Land use, land cover change and forestry (LULUCF).

For 2000–2019, despite a significant increase between the 2000s and the 2010s, the non-biospheric N₂O emissions from oil and gaseous fuel burning (0.026 Tg N₂O yr⁻¹) and waste disposal and burning (0.047 ± 0.032 Tg N₂O yr⁻¹) were significantly smaller than biospheric N₂O emissions, such as those from natural soils, agricultural soils, and manure management (Table 3). Consequently, those non-biospheric emissions contributed only modestly to the total N₂O budget (sum of the biospheric N₂O budget and non-biospheric emissions): 2.71 ± 0.71 Tg N₂O yr⁻¹ in the bottom-up approach and 1.54 ± 0.49 Tg N₂O yr⁻¹ in the top-down approach. The total N₂O budgets of both approaches increased between the 2000s and the 2010s with rates similar to those in the biospheric N₂O budgets (Table 3).

3.4. GHG Budget

For 2000–2019, the total biospheric GHG budget assessment (sum of the biospheric CO₂, CH₄, and N₂O budgets) revealed that the net contribution of Southeast Asia to the atmosphere was 2,003.2 ± 406.1 Tg CO₂eq yr⁻¹ (based on the bottom-up approach) and 2,227.5 ± 572.8 Tg CO₂eq yr⁻¹ (based on the top-down approach), respectively (Table 4). In both, the top-down and bottom-up approaches, all the individual budgets indicated that the region's biosphere was a net source of GHGs to the atmosphere, where in terms of the global warming potential, the biospheric CH₄ budget was the largest (bottom-up: 976.0 ± 203.2 Tg CO₂eq yr⁻¹; top-down: 1,253.1 ± 205.3 Tg CO₂eq yr⁻¹), followed by the biospheric N₂O budgets (bottom-up: 720.0 ± 194.5 Tg CO₂eq yr⁻¹; top-down: 363.1 ± 134.8 Tg CO₂eq yr⁻¹) and the biospheric CO₂ budgets (bottom-up: 308.1 ± 292.9 Tg CO₂eq yr⁻¹; top-down: 611.3 ± 517.5 Tg CO₂eq yr⁻¹), over the past two decades (Tables 4). The biospheric GHG budget increased toward a net source of 9% in the bottom-up estimate and 17% in the top-down estimate between the 2000s and the 2010s. This increase over the decades was common in all budgets and was most significant in the biospheric CO₂ budgets (bottom-up: 42%; top-down: 27%).

For 2000–2019, the total GHG budget of Southeast Asia, inclusive of non-biospheric GHG emissions from fossil fuels, waste, weathering uptake, and geological seepages, was calculated to be 3,226.3 ± 406.2 Tg CO₂eq yr⁻¹ (bottom-up approach) and 3,406.4 ± 572.9 Tg CO₂eq yr⁻¹ (top-down approach). In terms of the CO₂ equivalent, for 2000–2019, the non-biospheric CH₄ and N₂O emissions amounted to 185.1 and 19.90 Tg CO₂eq yr⁻¹, respectively, moderately increasing the net source of biospheric CH₄ and N₂O budgets by a maximum of 21% (Tables 2 and 3). During the same period, non-biospheric CO₂ emissions amounted to 1,107.0 Tg CO₂ yr⁻¹

Table 4

Bottom-Up and Top-Down Carbon Dioxide (CO₂), Methane (CH₄), Nitrous Oxide (N₂O), and Total Greenhouse Gas (GHG) Budget Estimates (Tg CO₂eq yr⁻¹) for Southeast Asia for the 2000s (2000–2009) and the 2010s (2010–2019) and 2000–2019

Budget	Approach type	2000s	2010s	2000–2019	Changes from the 2000s to the 2010s (%)
Biospheric CO ₂ budget	Bottom-up	253.6 ± 281.6	360.7 ± 304.3	308.1 ± 292.9	42
	Top-down	539.5 ± 344.6	683.2 ± 690.4	611.3 ± 517.5	27
Total CO ₂ budget	Bottom-up	1,018.0 ± 281.6	1,560.5 ± 304.3	1,289.3 ± 292.9	53
	Top-down	1,303.9 ± 344.6	1,883.0 ± 690.4	1,593.5 ± 517.5	44
Biospheric CH ₄ budget	Bottom-up	960.6 ± 201.3	991.5 ± 205.1	976.0 ± 203.2	3
	Top-down	1,181.7 ± 192.0	1,324.5 ± 218.6	1,253.1 ± 205.3	12
Total CH ₄ budget	Bottom-up	1,146.2 ± 201.5	1,248.0 ± 205.3	1,197.1 ± 203.4	9
	Top-down	1,292.4 ± 192.2	1,492.6 ± 218.8	1,392.5 ± 205.5	15
Biospheric N ₂ O budget	Bottom-up	703.9 ± 190.6	736.1 ± 198.3	720.0 ± 194.5	5
	Top-down	330.3 ± 112.9	395.9 ± 156.7	363.1 ± 134.8	20
Total N ₂ O budget	Bottom-up	720.5 ± 190.6	759.3 ± 198.3	739.9 ± 194.5	5
	Top-down	384.9 ± 112.9	455.9 ± 156.7	420.4 ± 134.8	18
Biospheric GHG budget	Bottom-up	1,918.7 ± 395.1	2,088.3 ± 417.2	2,003.2 ± 406.1	9
	Top-down	2,051.5 ± 410.3	2,403.5 ± 740.9	2,227.5 ± 572.8	17
Total GHG budget	Bottom-up	2,884.7 ± 395.2	3,567.9 ± 417.2	3,226.3 ± 406.2	24
	Top-down	2,981.2 ± 410.4	3,831.5 ± 741.0	3,406.4 ± 572.9	29

(Table 1), increasing the net source of the biospheric CO₂ budget by a maximum of four times. The increase in fossil fuel emissions facilitated almost all individual total budgets of CO₂, CH₄, and N₂O toward a net source between the 2000s and the 2010s, compared with those of the biospheric budgets (Table 4).

4. GHG Emissions of Anthropogenic Origin

Our GHG budget assessment revealed that Southeast Asia was a large net source of GHGs during 2000–2019, and the net source substantially increased between the 2000s and the 2010s, which makes achieving climate neutrality challenging for the region. As GHG emissions of anthropogenic origin are largely responsible for the region's total GHG budget being a net source of GHG (Tables 1–3), reducing and managing these emissions at low levels is a core part of planning a climate-neutral pathway in the region. Effective future reduction plans require a deep understanding of anthropogenic GHG emissions, assessed under two categories: those that originate in the biosphere, such as land-use changes, peat drainage, fires, agriculture, and livestock, and direct emissions from human activities, such as fossil fuel emissions and waste disposal and burning.

4.1. Anthropogenic GHG Emissions in the Biosphere

A comparison of anthropogenic CO₂, CH₄, and N₂O emissions in the biosphere revealed that gross FLUC emissions were the dominant component, exceeding other anthropogenic GHG emissions in the terms of warming potential (Figures 3a and 3b), highlighting the major effects of land-use changes on GHG emissions in Southeast Asia. CO₂ emissions from fires, including those from peat burning, were the 2nd largest GHG emission source, followed by CO₂ emissions from peat decomposition. The relative importance of these top three GHG emitters remained unchanged between the 2000s and the 2010s (Figures 3a and 3b). Among all CH₄-inducing anthropogenic activities considered in this study (e.g., agriculture, livestock, and fires), rice cultivation was the largest CH₄ emitter for the 2000s and the 2010s (Figures 3a and 3b) accounting for only 12% of the warming potential of the gross FLUC emissions. The dominant component of anthropogenic N₂O emissions, that is, agricultural soils, had a relatively small contribution to the warming potential during the 1990s and the 2010s, accounting for less than 5% of the gross FLUC emissions (Figures 3a and 3b).

Focusing on the top three anthropogenic GHG emitters in the biosphere (CO₂ emissions from FLUC, fires, and peat decomposition), we found that a large proportion of these emissions was concentrated in Indonesia among the nine major Southeast Asian countries evaluated (Figures 3c and 3d). In the 2000s and the 2010s, Indonesia

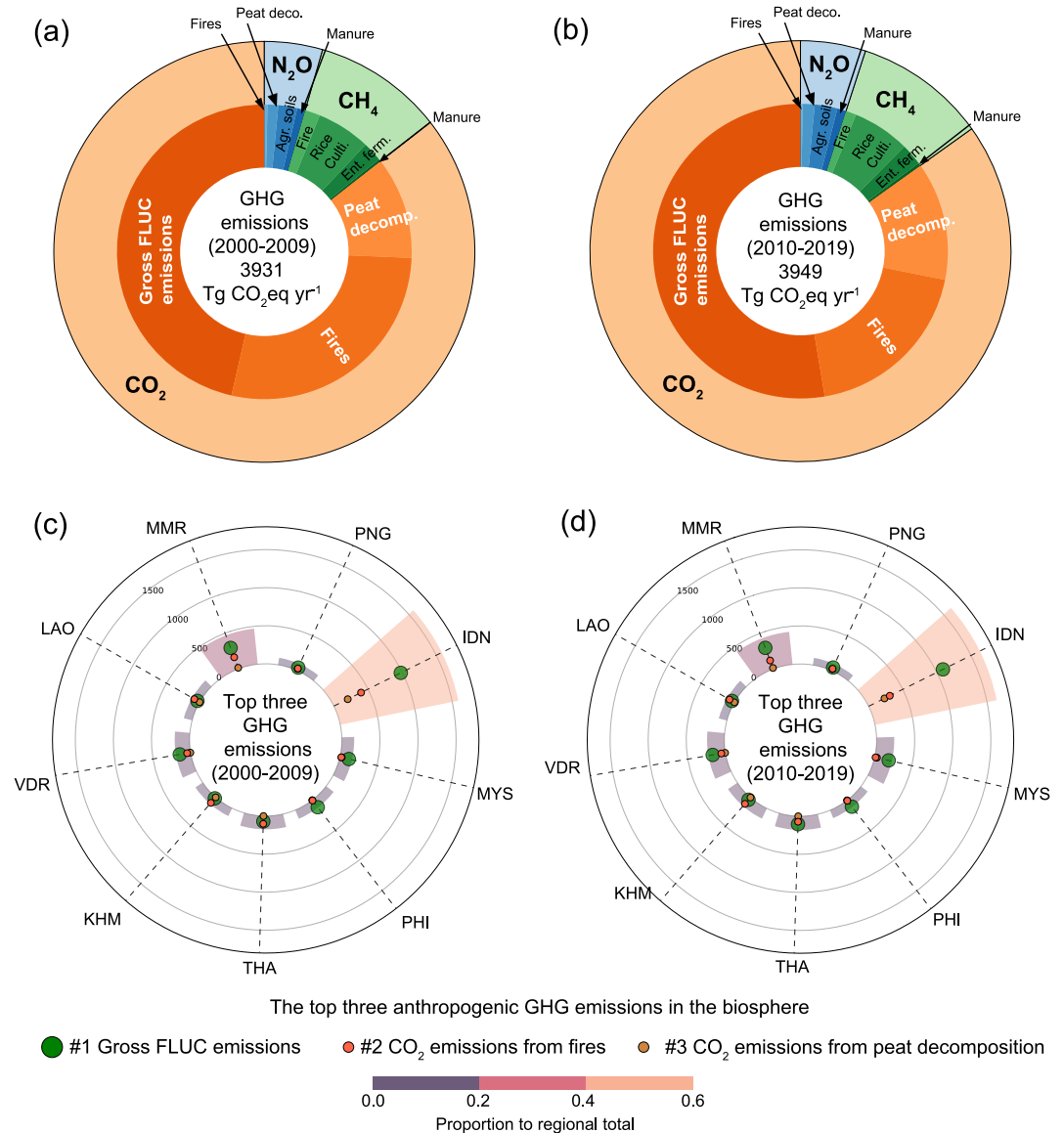


Figure 3. Decadal carbon dioxide (CO₂), methane (CH₄), and nitrous oxide (N₂O) emissions resulting from land use, land cover change and forestry (LULUCF), agriculture, and livestock. The proportions of anthropogenic greenhouse gas (GHG) emissions in the biosphere accounted for by CO₂, CH₄, and N₂O (outer circle) and their components (inner circle) are shown for (a) the 2000s and (b) the 2010s. “Fire” is the sum of emissions from peat fires and other types of fires. Proportions of the top three anthropogenic GHG emissions (gross forest land-use change (FLUC) emissions, CO₂ emissions from fires, and CO₂ emissions from peat decomposition) of the nine major Southeast Asian countries for (c) the 2000s and (d) the 2010s. The bars represent the proportion of each country to the regional total of the summed top three anthropogenic GHG emissions. Circles represent the proportion of each country to the regional total of the top three anthropogenic GHG emissions (green, gross FLUC emissions; red, CO₂ emissions from fires; and brown, CO₂ emissions from peat decomposition). Three letter country codes following ISO 3166-1 were used: Myanmar (MMR), Laos (LAO), Vietnam (VDR), Cambodia (KHM), Thailand (THA), the Philippines (PHI), Malaysia (MYS), and Indonesia (IND).

alone accounted for approximately 52% of these emissions in Southeast Asia, followed by Myanmar (~14%), and the rest of the countries contributed less than 10%. These proportions remained relatively unchanged between the 2000s and the 2010s. In these periods, gross FLUC emissions were the largest emissions in many countries, including Indonesia, Myanmar, Vietnam, Malaysia, Thailand (only in the 2010s), and the Philippines. Fire emissions were the largest in some continental countries, including Laos, Cambodia, and Thailand (only in the 2000s).

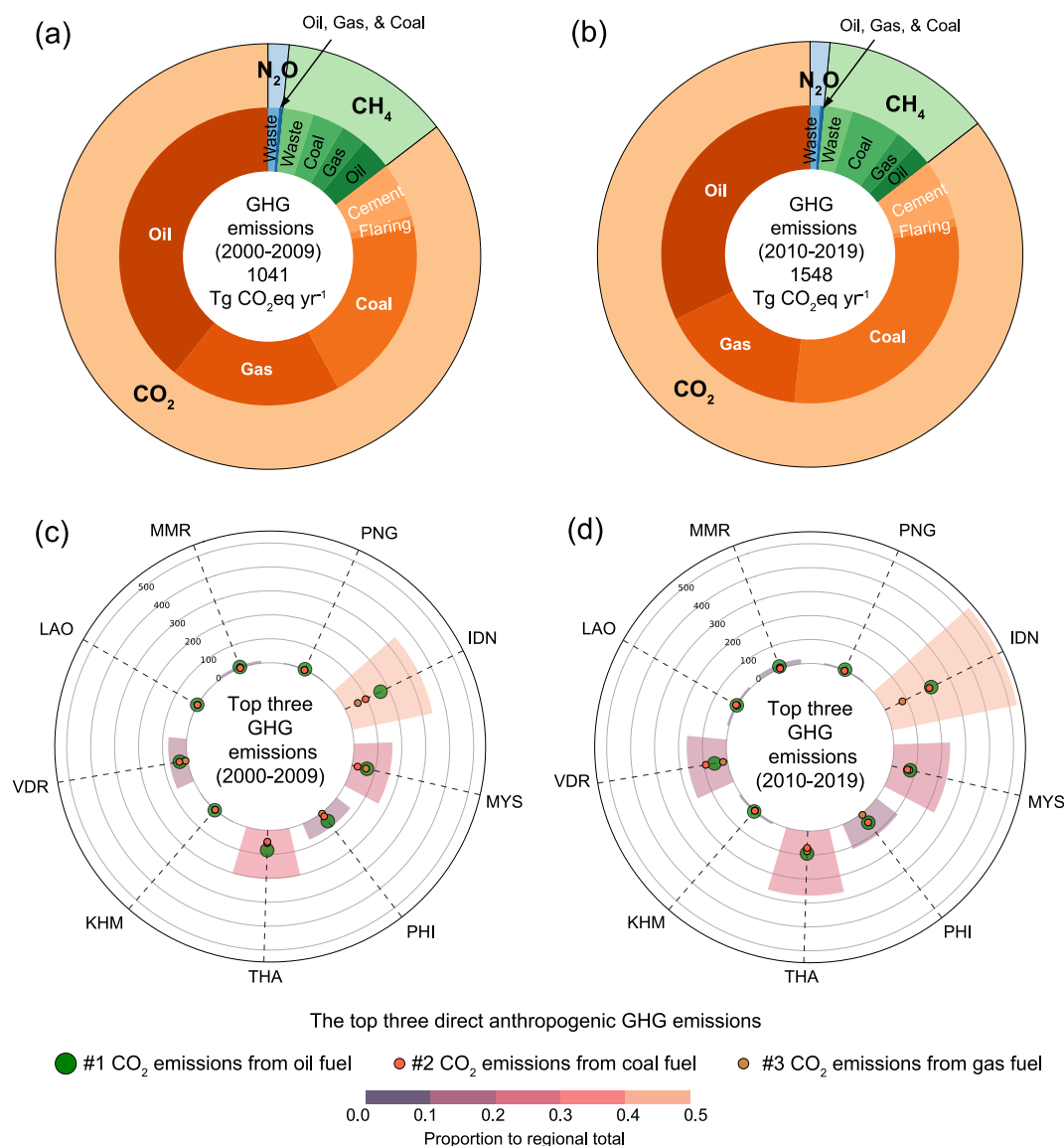


Figure 4. Decadal carbon dioxide (CO₂), methane (CH₄), and nitrous oxide (N₂O) emissions resulting from fossil fuel burning, exploitation, mining, and waste. The proportions of direct anthropogenic greenhouse gas (GHG) emissions accounted for by CO₂, CH₄, and N₂O (outer circle) and their components (inner circle) are shown for (a) the 2000s and (b) the 2010s. Proportions of the top three direct anthropogenic CO₂ emissions (CO₂ emissions from oil, coal, and gas fuels) of the nine major Southeast Asian countries for (c) the 2000s and (d) the 2010s. The bars represent the proportion of each country to the regional total of the summed top three direct anthropogenic CO₂ emissions. Circles represent the proportion of each country to the regional total of the top three direct anthropogenic CO₂ emissions (green, CO₂ emissions from oil fuels; red, CO₂ emissions from coal fuels; and brown; CO₂ emissions from gas fuels). Three letter country codes following ISO 3166-1 were used: Myanmar (MMR), Laos (LAO), Vietnam (VDR), Cambodia (KHM), Thailand (THA), the Philippines (PHI), Malaysia (MYS), and Indonesia (IND).

4.2. GHG Emissions From Fossil Fuels and Waste

Among all the GHG emissions from fossil fuels and waste in the region, CO₂ emissions from oil fuels were a major component in the 2000s, accounting for 40%, followed by CO₂ emissions from coal fuels (21%), and gas fuels (19%) (Figure 4a). The order of the top three GHG emitters did not change between the 2000s and the 2010s, but the proportion of CO₂ emissions from coal fuels in the total CO₂ emissions increased to 30%, whereas those of oil and gas fuels were reduced to 32% and 16%, respectively (Figures 4a and 4b). In the 2000s, CH₄ emissions from oil extraction, coal mining, and waste accounted for equivalent proportions (~26%) of the total

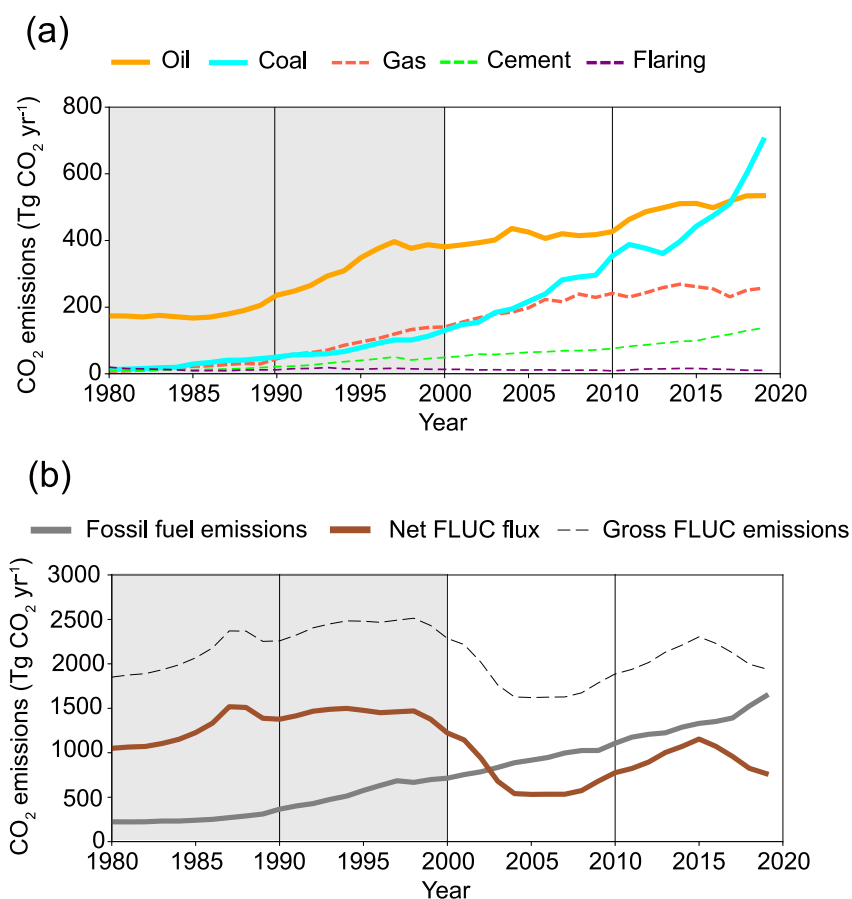


Figure 5. Interannual variation in anthropogenic carbon dioxide (CO_2) emissions contributed significantly to the GHG budget, from 1980 to 2019. (a) Interannual variability in CO_2 emissions from oil, gas, coal fuels, cement production, and gas flaring for 1980 to 2019. Two key emissions, CO_2 emissions from oil and coal fuels, are shown by bold lines, and the rest are represented by dashed lines. (b) Interannual variability in net LUC flux, gross LUC emissions (dashed line), and total fossil fuel CO_2 emissions (sum of CO_2 emissions from oil, gas, coal fuels, cement production, and gas flaring). The period prior to the target period for the GHG budget assessment is shown in gray shading.

anthropogenic CH_4 emissions, but the emissions from coal mining became dominant (42%) in the 2010s. Among N_2O emissions, waste-related N_2O emissions remained the largest component (65%) throughout the 2000s and the 2010s, displacing fossil fuel emissions. Nevertheless, these major CH_4 and N_2O emissions were substantially smaller than the CO_2 emissions from oil and coal fuels (less than 10%).

Among the nine major Southeast Asian countries, a large proportion of the top three GHG emissions from fossil fuels and waste (CO_2 emissions from oil, coal, and gas fuels) was found in Indonesia (~40%), followed by Thailand (~20%), Malaysia (~18%), Vietnam (~10%), and the Philippines (~8%) (Figures 4c and 4d). The order of these countries remained unchanged, although the top three emissions together increased by approximately $480 \text{ TgCO}_2 \text{ yr}^{-1}$. CO_2 emissions from oil fuels were the largest in all countries during the 2000s, except for Vietnam. This pattern remained the same during the 2010s, except that CO_2 emissions from coal fuel became the largest in Laos. Common to all countries, CO_2 emissions from coal fuels increased between the 2000s and the 2010s, with their decadal estimates in the 2010s becoming close to those from oil fuels.

4.3. Transitions of Anthropogenic GHG Emissions

The detailed investigation of anthropogenic GHG emissions highlights the evolving GHG emission landscape in Southeast Asia, revealing major emissions that characterize the net source of the current GHG budget in the region: CO_2 emissions from land-use changes in forests and from oil and coal fuels. Looking back from 1980 to 2019, CO_2 emissions from oil fuels dominated the rest from 1980 to 1999, with a continuously increasing pattern

(Figure 5a). However, even the total CO₂ emissions from fossil fuels, including oil, gas, and coal fuels, cement production, and gas flaring, were significantly lower than those from land-use changes in forests (gross FLUC emissions and net FLUC flux) during the same period, indicating that land-use changes in forests was by far the GHG emission source that most characterizes Southeast Asia in the past (Figure 5b).

Emissions from oil fuels increased from the 1980s through the late 1990s but remained relatively stable until the late 2000s, after which the rate of increase slowed until 2019 (Figure 5b). In contrast, CO₂ emissions from coal fuels have increased sharply since 2005 with an unprecedented rate of growth in the energy sector, surpassing CO₂ emissions from oil fuels in 2018 (Figure 5a). This suggests that coal fuels may become a major source of fossil fuel emissions in Southeast Asia in the near future. The shift from oil to coal use during 2000–2019 resulted in a continued increase in total CO₂ emissions from fossil fuels (Figure 5b).

The gross CO₂ emissions from land-use changes in forests, which were the largest source of GHG emissions in the region from 2000 to 2019, had even higher values for the long period from 1980 to 1999 (Figure 5b). It then declined significantly throughout the 2000s, and gradually increased from the late 2000s to the 2010s. In other words, focusing only on the period covered by this study, 2000–2019, it appears that land-use changes in forests simply became more active over the course of 20 years, but in fact, it was in a state of reactivity after recovering from the most active period in the 1990s.

These results suggest that a pivotal period for Southeast Asia was the 2000s, marked by stable CO₂ emissions from oil fuels (Figure 5a) and a significant reduction in gross FLUC emissions compared with the emissions released in the 1990s (Figure 5b). A previous study suggested that the decrease in gross FLUC emissions was due to economic factors, such as the Asian economic crisis of 1997–1998 and Indonesia's shift from wood production to plantations, which played a pivotal role in slowing down the loss of primary forests (Kondo et al., 2022). If Southeast Asian countries took advantage of this situation and initiated large-scale deforestation reduction and reforestation programs, the lower levels of CO₂ emissions in the 2000s (Figure 5b) could have persisted and even improved. Similarly, if Southeast Asian countries decided in the 2000s to shift their energy sources away from coal fuels and toward more efficient and cleaner natural gas and alternative energy resources, the increasing trend in CO₂ emissions could have been lowered.

However, CO₂ emissions from fossil fuels and land-use changes in forests showed a parallel increase during the 2010s (Figure 5b), which was enhanced by the rise in CO₂ emissions from coal fuels and the resumption of deforestation. Notably, although gross FLUC emissions were still dominant, the total CO₂ emissions from fossil fuels surpassed the net FLUC flux (inclusive of gross FLUC uptake) in the early 2000s, suggesting a transition from forestry to industry in Southeast Asia's economies. Recent findings based on the Global Energy Monitor (<https://globalenergymonitor.org/projects/global-coal-plant-tracker/>) revealed a concerning scenario. If all planned and under-constructed coal plants as of 2020 were to be operationalized, GHG emissions from the power sector in Southeast Asia could increase by 72% from 2020 to 2030 (Chen & Mauzerall, 2021). While it is unclear whether the increase in land-use changes in forests in the 2010s was temporary, it is necessary to monitor and sustain its associated CO₂ emissions so that they do not revert to those of the 1990s.

5. Uncertainty in GHG Budget Estimates

In this study, we strived to provide a comprehensive assessment of all major anthropogenic and natural sources and sinks of the three most important GHGs. We acknowledge that our budget estimates and fluxes comprising the GHG budget contained large uncertainties. One of the main issues with the GHG budget assessment for Southeast Asia is that local-scale dynamics may not be fully reflected in the estimates, owing to the lack of region-specific data. For example, in all peat-related GHG flux estimates, peatlands were treated and characterized as being static. However, the extent of peatlands in Southeast Asia has undergone dynamic changes owing to various anthropogenic influences over the past few decades. A recent study reported a peatland extent of approximately 13 Mha in Indonesia, indicating a reduction in its extent from the formerly reported area of 15–27 Mha (Anda et al., 2021). This large variability has significant implications for the quantification of GHG emissions released from fires and drained peatlands. Oil palm and rubber plantations are another set of key factors that characterize GHG emissions in Southeast Asia (Melton et al., 2022; Wang et al., 2023). However, they were classified together with other plantations for FLUC flux estimation (i.e., H&C), without reflecting the high productivity of these plantations in significantly shaping the estimates. The GHG fluxes of coastal ecosystems, particularly mangrove

forests and seagrass meadows, are known to contain large carbon stocks per unit area (Bouillon et al., 2008); however, to date, their GHG fluxes have been poorly quantified.

The impact of fire emissions on GHG budgets may be lower than that indicated in this study. Extreme drought conditions associated with El Niño events have been identified as triggers for large and abrupt GHG emissions in Southeast Asia (Huijnen et al., 2016; Lohberger et al., 2017; Page et al., 2002; Siebert et al., 2001; Thirumalai et al., 2017; Vadrevu et al., 2019). Among the ENSO-sensitive fluxes, biomass burning, including peat burning is known to induce anomalous GHG emissions in the region (Page et al., 2002; Page & Hooijer, 2016). However, despite these well-known fire events in the region, independent atmospheric inverse model experiments, one using the column-average dry air-mole fraction of CO₂ from the Orbiting Carbon Observatory-2 (OCO-2) (Heymann et al., 2017) and the other utilizing CO₂ measurements from aircraft and ships over Southeast Asia (Niwa et al., 2021), reported that CO₂ emissions from fires in equatorial Southeast Asia during 2015 to be approximately 30% lower than those reported by GFEDv4s.

The natural vegetation flux (NEE), which was estimated through the TRENDY S2 simulation (no LULUCF effect), was the largest net sink component among all the GHG fluxes considered in this study; however, the range of the estimates was proportionally large (Table 1), implying that model sensitivity to atmospheric CO₂ and climate in the models is still a factor that confounds attempts to accurately estimate the GHG budget of Southeast Asia. Additionally, the natural vegetation flux represented by the TRENDY S2 simulation included the net CO₂ sink of undisturbed ecosystems, which should have been affected by LULUCF. Therefore, our estimate of the net CO₂ sink by natural vegetation may be partially overestimated by the uptake by non-existent natural ecosystems. Similarly, the wetland CH₄ emissions and natural soil N₂O fluxes, both based on process-based models, were the largest emission components of the CH₄ and N₂O budgets, with proportionally large uncertainties (Tables 2 and 3). Thus, reducing the estimation range of process-based models is the key to reducing the uncertainty of the GHG budget in the bottom-up approach. Although the contributions to the GHG budget were small, we need to address the wide range of estimates for global emission inventories, as evidenced by the estimates of CH₄ and N₂O emissions from agriculture and livestock (Tables 2 and 3).

In Southeast Asia, a region where atmospheric observations are scarce, the GHG fluxes estimated via atmospheric inversions inevitably have uncertainties embedded within them. In such situations, column-averaged CO₂ observations from satellites are expected to improve top-down GHG flux estimates. However, column-averaged GHG observations have their own issues regarding spatial biases, producing larger net sinks in northern temperate and boreal regions and larger net sources in tropical regions when assimilated into atmospheric inversions (Byrne et al., 2023; Houweling et al., 2015). In addition to the issue of data assimilation, an experiment conducted with MIROC4-ACTM revealed that the choice of prior land and ocean fluxes produced large regional sink/source variability (Chandra et al., 2022). The underlying reasons for the uncertainties in atmospheric inversions could be attributed to the fundamental model features, including the model resolution, control vector size, assimilation window length, transport model errors, and land-ocean separation (Kondo et al., 2020).

6. A Way Forward to Achieving Climate Neutrality

This study is the first to estimate the GHG budget for Southeast Asia, including all major anthropogenic and natural sources and sinks of CO₂, CH₄, and N₂O. We show that the region is a large net source of GHG, ranging from $3,226.3 \pm 406.2$ Tg CO₂eq yr⁻¹ to $3,406.4 \pm 572.9$ Tg CO₂eq yr⁻¹ for 2000–2019. We identified that the large net source of the GHG budget was largely driven by anthropogenic CO₂ emissions, such as land-use changes in forests and fossil fuels. Looking ahead to future energy policies within the context of the ASEAN region, the Long-range Energy Alternatives Planning model envisions a climate-neutral scenario, aiming to achieve climate neutrality (neutrality of all GHGs) by 2050 (Handayani et al., 2022). However, based on our estimates, the LEAPS model goal is not realistic, as it is unlikely that the increasing anthropogenic GHG emissions can be turned around quickly enough, and the remaining emissions will be offset over the next 25 years. Realistically, to meet the 1.5°C threshold target, in line with the scenarios proposed by the IPCC, effective plans should be implemented to achieve net-zero CO₂ emissions by 2050 and complete net-zero GHG emissions (including net-zero CH₄ and N₂O emissions) by 2070. Currently, some Southeast Asian countries are committed to achieving net-zero emissions by 2050 (e.g., Vietnam and Malaysia), and some of the largest emitters have set this target to 2060–65 (e.g., Indonesia and Thailand).

The results of this study will help to effectively plan and set reduction targets that focus on sources with particularly high emissions rather than addressing all emission sources within a limited timeframe. CH₄ and N₂O emissions from agriculture and livestock sectors can be reduced by adopting precision agriculture, improving livestock management, and implementing sustainable agricultural practices. However, according to our assessment, GHG emissions from those sectors during 2000–2019 amounted to 466.0 Tg CO_{2eq} yr⁻¹, accounting for only 20% of the gross FLUC emissions. Instead, a more effective plan would focus on reducing CO₂ emissions from land-use changes in forests and fossil fuels, the most significant sources of GHG emissions in the region (totaling 3,058.5 Tg CO₂ yr⁻¹ during 2000–2019), as reducing approximately 30% of these emissions offsets all anthropogenic CH₄ and N₂O emissions combined, including CH₄ and N₂O emissions from agriculture, livestock, peat drainage, and fires. Furthermore, limiting land-use changes in forests may promote ecosystem regeneration and lead to increased CO₂ uptake. Currently, land-use changes in Southeast Asia are a net source of GHGs, with emissions far exceeding the uptake by ecosystem regrowth and afforestation (Table 1). In northern temperate regions, the absence of land uses (abandonment of cropland) has resulted in hotspots of CO₂ uptake owing to the recovery of natural vegetation (Kondo, Ichii, Patra, Poulter, et al., 2018; Pugh et al., 2019). It may be possible to induce hotspots of CO₂ uptake in Southeast Asia by promoting afforestation, in addition to limiting land-use changes such as wood harvesting and shifting cultivation, thereby restoring the region's naturally productive forests. GHG emissions from fires should also be included as reduction targets for Southeast Asia. This is not only because fires are the second largest source of CO₂ emissions after land-use changes in forests, but also they remain a major environmental and social issue in Southeast Asian countries, leading to high concentrations of pollutants being released into the atmosphere (causing hazardous haze), posing a threat to human health, aviation, and the environmental well-being of the region (Crippa et al., 2016; Othman et al., 2022; Tan-Soo & Pattanayak, 2018).

To make these reduction targets a reality, it is essential to address uncertainties and refine GHG budget estimates in Southeast Asia so that they can be downscaled to a national scale. Southeast Asian countries are diverse in terms of climate, vegetation distribution, and economic development; therefore, their GHG budgets and mitigation opportunities vary significantly. As this study shows, Indonesia, which is responsible for much of the CO₂ emissions from land-use changes in forests and fossil fuels (Figures 3c, 3d, 4c, and 4d), must play a central role in achieving climate neutrality in Southeast Asia as a whole. However, we note that mitigation and net-zero emission targets under the Paris Agreement are nationally determined, and therefore, the responsibility for achieving them lies with individual nation-states. In contrast to developed countries, where fossil fuels account for the majority of GHG emissions, Southeast Asia is undergoing rapid economic development, making it particularly challenging to pursue a pathway that achieves climate neutrality and sustained economic growth.

Even with the latest data set prepared by RECCAP2, some of the data are statistical estimates that only cover the entire region of Southeast Asia and cannot be downscaled into detailed values on a national scale. To overcome these challenges, we launched an international network to facilitate the quantification of GHG fluxes in Southeast Asia, namely, the League of geophysical research eXcellences for tropical Asia (LeXtra). LeXtra continues to improve GHG fluxes and monitoring in Southeast Asia's GHG budget, while enabling the identification of the detailed contributions from each country in Southeast Asia, which could not be addressed in this study. This effort will be supported and be a contribution to the Global Carbon Project's new REgional Carbon Cycle Assessment and Processes, Phase 3 (RECCAP3), which will particularly focus on national-level GHG budgets (Canadell et al., 2025).

Conflict of Interest

The authors declare no conflicts of interest relevant to this study.

Data Availability Statement

All data used in this study are publicly available from the data repository of RECCAP-2 (<https://www.bgc-jena.mpg.de/geodb/projects/Home.php>), the Global Carbon Budget 2022 (Friedlingstein et al., 2022), IEA2023 (<https://www.iea.org/>), EDGARv7.0 (https://edgar.jrc.ec.europa.eu/dataset_ghg70), CEDSv2021 (<https://zenodo.org/records/4741285>), FAOSTAT (<http://www.fao.org/faostat/en/#data>), and individual sources. Weathering CO₂ uptake, book-keeping estimates of gross FLUC emissions and uptake, river carbon exports, coastal

vegetation fluxes, wood and crop trade, wetland CH₄ emissions, N₂O fluxes of natural soils, and a majority of CO₂, CH₄, and N₂O inversions are available from the data repository of RECCAP-2. CO₂ and CH₄ emissions from oil, coal, and gas are available from IEA2023, and N₂O emissions from oil, coal, and gas, are available from EDGARv7.0. CO₂ emissions from Cement production and gas flaring are available from the Global Carbon Budget 2022. CH₄ and N₂O emissions from waste disposal and burning are available from EDGARv7.0 and CEDSV2021. GHG emissions from manure management, enteric fermentation, rice cultivation, and agricultural soils are available from FAOSTAT, EDGARv7.0, and CEDSV2021. GHG emissions from fire are available from FAOSTAT and GFEDs4.1 (<https://www.globalfiredata.org/data.html>). Geological seepage data are available from Etiopé et al. (2019) (<https://gml.noaa.gov/ccgg/arc/index.php?id=130>). CO₂, CH₄ and N₂O outgassing from lakes and rivers are available from Lauerwald et al. (2023) (<https://doi.org/10.6084/m9.figshare.22492504>). TRENDY data are available via Profs. Stephen Sitch and Pierre Friedlingstein, Exeter University (s.a.sitch@exeter.ac.uk; p.friedlingstein@exeter.ac.uk). VISIT simulations for oxidative CH₄ consumption and termite CH₄ emissions are available via Prof. Akihiko Ito, the Tokyo University (akihikoito@g.ecc.u-tokyo.ac.jp). Three CO₂ inversions, ACTM_CONTRAIL, JMA2021, and GOSAT L4A are available via Dr. Tazu Saeki (saeki.tazu@nies.go.jp), Dr. Takashi Maki (tmaki@mri-jma.go.jp), and from the GOSAT data portal (https://data2.gosat.nies.go.jp/index_en.html), respectively. All data sets used in this study were listed in Tables S1–S6 in Supporting Information S1 with detailed data descriptions and link for access.

Acknowledgments

This paper is a contribution to the Regional Carbon Cycle Assessment and Processes (RECCAP) Phase 2 coordinated by the Global Carbon Project, and to the League of geophysical research eXcellences for tropical Asia (LeXtra) sponsored by Integrated Land Ecosystem-Atmosphere Processes Study (iLEAPS). P.K.P. and N.C. were supported by the Arctic Challenge for Sustainability II (ArCS-II) project (Grant JPMXD1420318865), funded by Japan's Ministry of Education, Culture, Sports, Science and Technology (MEXT). A.I. was supported by the Environmental and Technology Development Fund (JPMEERF21S20800) of the Environmental Restoration and Conservation Agency of Japan. T.M. was supported by the JSPS KAKENHI (Grant numbers: JP19K12312), Environment Research and Technology Development Fund (JPMEERF21S20810) of the Environmental Restoration and Conservation Agency of Japan from the Ministry of the Environment, Japan. R.L. acknowledges funding from French state aid, managed by ANR under the "Investissements d'avenir" programme (ANR-16-CONV-0003). A. K. J. was supported by NASA LCLUC program (grant number: 80NSSC24K0920). We express our deep gratitude to all the researchers who were involved in this research and RECCAP2 through project management, data provision, and discussions.

References

- Achard, F., Beuchle, R., Mayaux, P., Stibig, H.-J., Bodart, C., Brink, A., et al. (2014). Determination of tropical deforestation rates and related carbon losses from 1990 to 2010. *Global Change Biology*, 20(8), 2540–2554. <https://doi.org/10.1111/gcb.12605>
- Allen, G. H., & Pavelsky, T. M. (2018). Global extent of rivers and streams. *Science*, 361(6402), 585–588. <https://doi.org/10.1126/science.aat0636>
- Anda, M., Ritung, S., Suryani, E., Hikmat, M., Yatno, E., Mulyani, A., et al. (2021). Revisiting tropical peatlands in Indonesia: Semi-detailed mapping, extent and depth distribution assessment. *Geoderma*, 402, 115235. <https://doi.org/10.1016/j.geoderma.2021.115235>
- Andrew, R. M. (2018). Global CO₂ emissions from cement production. *Earth System Science Data*, 10(1), 195–217. <https://doi.org/10.5194/essd-10-195-2018>
- Baccini, A., Walker, W., Carvalho, L., Farina, M., Sulla-Menashe, D., & Houghton, R. A. (2017). Tropical forests are a net carbon source based on aboveground measurements of gain and loss. *Science*, 358(6360), 230–234. <https://doi.org/10.1126/science.aam5962>
- Bergamaschi, P., Houweling, S., Segers, A., Krol, M., Frankenberg, C., Scheepmaker, R. A., et al. (2013). Atmospheric CH₄ in the first decade of the 21st century: Inverse modeling analysis using SCIAMACHY satellite retrievals and NOAA surface measurements. *Journal of Geophysical Research-Atmospheres*, 118(13), 7350–7369. <https://doi.org/10.1002/jgrd.50480>
- Bouillon, S., Borges, A. V., Castañeda-Moya, E., Diele, K., Dittmar, T., Duke, N. C., et al. (2008). Mangrove production and carbon sinks: A revision of global budget estimates. *Global Biogeochemical Cycles*, 22, GB2013. <https://doi.org/10.1029/2007GB003052>
- Byrne, B., Baker, D. F., Basu, S., Bertolacci, M., Bowman, K. W., Carroll, D., et al. (2023). National CO₂ budgets (2015–2020) inferred from atmospheric CO₂ observations in support of the global stocktake. *Earth System Science Data*, 15(2), 963–1004. <https://doi.org/10.5194/essd-15-963-2023>
- Cai, W., Wu, L., Lengaigne, M., Li, T., McGregor, S., Kug, J.-S., et al. (2019). Pantropical climate interactions. *Science*, 363, 6430. <https://doi.org/10.1126/science.aav4236>
- Canadell, J. G., Monteiro, P. M., Costa, M. H., Da Cunha, L. C., Cox, P. M., Alexey, V., et al. (2021). Global carbon and other biogeochemical cycles and feedbacks. In V. Masson-Delmotte, P. Zhai, A. Pirani, S. L. Connors, C. Péan, S. Berger, et al. (Eds.), *Climate change 2021: The physical science basis. Contribution of working group I to the sixth assessment report of the intergovernmental Panel on climate change* (pp. 673–816). Cambridge University Press. <https://doi.org/10.1017/9781009157896.007>
- Canadell, J. G., Poulter, B., Bastos, A., Ciais, P., Hauck, J., Andrew, R., et al. (2025). From global to national GHG budgets: The Regional carbon cycle assessment and processes-3 (RECCAP3). *National Science Review*, 12(4), nwaf037. <https://doi.org/10.1093/nsr/nwaf037>
- Carlson, K. M., Curran, L. M., Ratnasari, D., Pittman, A. M., Soares-Filho, B. S., Asner, G. P., et al. (2012). Committed carbon emissions, deforestation, and community land conversion from oil palm plantation expansion in West Kalimantan, Indonesia. *Proceedings of the National Academy of Sciences of the United States of America*, 109(19), 7559–7564. <https://doi.org/10.1073/pnas.1200452109>
- Carlson, K. M., Heilmayr, R., Gibbs, H. K., Noojipady, P., Burns, D. N., Morton, D. C., et al. (2018). Effect of oil palm sustainability certification on deforestation and fire in Indonesia. *Proceedings of the National Academy of Sciences of the United States of America*, 115(1), 121–126. <https://doi.org/10.1073/pnas.1704728114>
- Chandra, N., Patra, P. K., Bisht, J. S. H., Ito, A., Umezawa, T., Saigusa, N., et al. (2021). Emissions from the oil and gas sectors, coal mining and ruminant farming drive methane growth over the past three decades. *Journal of the Meteorological Society of Japan. Ser. II*, 99(2), 309–337. <https://doi.org/10.2151/jmsj.2021-015>
- Chandra, N., Patra, P. K., Niwa, Y., Ito, A., Iida, Y., Goto, D., et al. (2022). Estimated regional CO₂ flux and uncertainty based on an ensemble of atmospheric CO₂ inversions. *Atmospheric Chemistry and Physics*, 22(14), 9215–9243. <https://doi.org/10.5194/acp-22-9215-2022>
- Chen, X., & Mauzerall, D. L. (2021). The expanding coal power fleet in Southeast Asia: Implications for future CO₂ emissions and electricity generation. *Earth's Future*, 9(12), e2021EF002257. <https://doi.org/10.1029/2021EF002257>
- Chevallier, F., Ciais, P., Conway, T. J., Aalto, T., Anderson, B. E., Bousquet, P., et al. (2010). CO₂ surface fluxes at grid point scale estimated from a global 21 year reanalysis of atmospheric measurements. *Journal of Geophysical Research*, 115(D21), D21307. <https://doi.org/10.1029/2010JD013887>
- Chini, L., Hurtt, G., Sahajpal, R., Frolking, S., Klein Goldewijk, K., Sitch, S., et al. (2021). Land-use harmonization datasets for annual global carbon budgets. *Earth System Science Data*, 13(8), 4175–4189. <https://doi.org/10.5194/essd-13-4175-2021>
- Ciais, P., Bastos, A., Chevallier, F., Lauerwald, R., Poulter, B., Canadell, J. G., et al. (2022). Definitions and methods to estimate regional land carbon fluxes for the second phase of the REGIONAL Carbon Cycle Assessment and Processes Project (RECCAP-2). *Geoscientific Model Development*, 15(3), 1289–1316. <https://doi.org/10.5194/gmd-15-1289-2022>

- Crippa, M., Guizzardi, D., Pagani, F., Banja, M., Muntean, M., Schaaf, E., et al. (2023). *GHG emissions of all world countries*. Publications Office of the European Union. JRC134504. <https://doi.org/10.2760/953322>
- Crippa, P., Castruccio, S., Archer-Nicholls, S., Lebron, G. B., Kuwata, M., Thota, A., et al. (2016). Population exposure to hazardous air quality due to the 2015 fires in Equatorial Asia. *Scientific Reports*, 6(1), 37074. <https://doi.org/10.1038/srep37074>
- Curry, C. L. (2007). Modeling the soil consumption of atmospheric methane at the global scale. *Global Biogeochemical Cycles*, 21(4), GB4012. <https://doi.org/10.1029/2006GB002818>
- Etiopie, G., Ciotoli, G., Schwietzke, S., & Schoell, M. (2019). Gridded maps of geological methane emissions and their isotopic signature. *Earth System Science Data*, 11, 1–22. <https://doi.org/10.5194/essd-11-1-2019>
- Feng, L., Palmer, P. I., Parker, R. J., Deutscher, N. M., Feist, D. G., Kivi, R., et al. (2016). Estimates of European uptake of CO₂ inferred from GOSAT XCO₂ retrievals: Sensitivity to measurement bias inside and outside Europe. *Atmospheric Chemistry and Physics*, 16(3), 1289–1302. <https://doi.org/10.5194/acp-16-1289-2016>
- Field, R. D., van der Werf, G. R., & Shen, S. S. P. (2009). Human amplification of drought-induced biomass burning in Indonesia since 1960. *Nature Geoscience*, 2(3), 185–188. <https://doi.org/10.1038/ngeo443>
- Food and Agriculture Organization (FAO). (2020). *Global forest resources assessment 2020: Main report*, Rome, Italy.
- Forster, P., Storelvmo, T., Armour, K., Collins, W., Dufresne, J.-L., Frame, D., et al. (2021). The Earth's energy budget, climate feedbacks, and climate sensitivity. In V. Masson-Delmotte, P. Zhai, A. Pirani, S. L. Connors, C. Péan, S. Berger, et al. (Eds.), *Climate change 2021: The physical science basis. Contribution of working group I to the sixth assessment report of the intergovernmental Panel on climate change* (pp. 923–1054). Cambridge University Press. <https://doi.org/10.1017/9781009157896.009>
- Friedlingstein, P., Jones, M. W., O'Sullivan, M., Andrew, R. M., Bakker, D. C. E., Hauck, J., et al. (2022). Global carbon budget 2021. *Earth System Science Data*, 14(4), 1917–2005. <https://doi.org/10.5194/essd-14-1917-2022>
- Giglio, L., Boschetti, L., Roy, D. P., Humber, M. L., & Justice, C. O. (2018). The Collection 6 MODIS burned area mapping algorithm and product. *Remote Sensing of Environment*, 217, 72–85. <https://doi.org/10.1016/j.rse.2018.08.005>
- Handayani, K., Anugrah, P., Goembira, F., Overland, I., Suryadi, B., & Swandaru, A. (2022). Moving beyond the NDCs: ASEAN pathways to a net-zero emissions power sector in 2050. *Applied Energy*, 311, 118580. <https://doi.org/10.1016/j.apenergy.2022.118580>
- Hansis, E., Davis, S. J., & Pongratz, J. (2015). Relevance of methodological choices for accounting of land use change carbon fluxes. *Global Biogeochemical Cycles*, 29(8), 1230–1246. <https://doi.org/10.1002/2014gb004997>
- Hartmann, J., Jansen, N., Dürr, H. H., Kempe, S., & Köhler, P. (2009). Global CO₂-consumption by chemical weathering: What is the contribution of highly active weathering regions? *Global and Planetary Change*, 69(4), 185–194. <https://doi.org/10.1016/j.gloplacha.2009.07.007>
- Heymann, J., Reuter, M., Buchwitz, M., Schneising, O., Bovensmann, H., Burrows, J. P., et al. (2017). CO₂ emission of Indonesian fires in 2015 estimated from satellite-derived atmospheric CO₂ concentrations. *Geophysical Research Letters*, 44(3), 1537–1544. <https://doi.org/10.1002/2016GL072042>
- Hooijer, A., Page, S., Canadell, J. G., Silvius, M., Kwadijk, J., Wösten, H., & Jauhiainen, J. (2010). Current and future CO₂ emissions from drained peatlands in Southeast Asia. *Biogeosciences*, 7(5), 1505–1514. <https://doi.org/10.5194/bg-7-1505-2010>
- Hooijer, A., Page, S., Jauhiainen, J., Lee, W. A., Lu, X. X., Idris, A., & Anshari, G. (2012). Subsidence and carbon loss in drained tropical peatlands. *Biogeosciences*, 9(3), 1053–1071. <https://doi.org/10.5194/bg-9-1053-2012>
- Houghton, R. A., & Castanho, A. (2023). Annual emissions of carbon from land use, land-use change, and forestry from 1850 to 2020. *Earth System Science Data*, 15(5), 2025–2054. <https://doi.org/10.5194/essd-15-2025-2023>
- Houghton, R. A., & Nassikas, A. A. (2017). Global and regional fluxes of carbon from land use and land cover change 1850–2015. *Global Biogeochemical Cycles*, 31(3), 456–472. <https://doi.org/10.1002/2016GB005546>
- Houweling, S., Baker, D., Basu, S., Boesch, H., Butz, A., Chevallier, F., et al. (2015). An intercomparison of inverse models for estimating sources and sinks of CO₂ using GOSAT measurements. *Journal of Geophysical Research-Atmosphere*, 120(10), 5253–5266. <https://doi.org/10.1002/2014JD022962>
- Huijnen, V., Wooster, M. J., Kaiser, J. W., Gaveau, D. L. A., Flemming, J., Parrington, M., et al. (2016). Fire carbon emissions over maritime southeast Asia in 2015 largest since 1997. *Scientific Reports*, 6(1), 26886. <https://doi.org/10.1038/srep26886>
- IPCC. (2006). In H. S. Eggleston, L. Buendia, K. Miwa, T. Ngara, & K. Tanabe (Eds.), *2006 IPCC guidelines for national greenhouse gas inventories, prepared by the national greenhouse gas inventories programme*. IGES.
- IPCC. (2014). In T. Hiraishi, T. Krug, K. Tanabe, N. Srivastava, J. Baasansuren, M. Fukuda, & T. G. Troxler. (Eds.), *2013 supplement to the 2006 IPCC guidelines for national greenhouse gas inventories: Wetlands*. IPCC. Switzerland.
- Ishizawa, M., Mabuchi, K., Shirai, T., Inoue, M., Morino, I., Uchino, O., et al. (2016). Interannual variability of summertime CO₂ exchange in Northern Eurasia inferred from GOSAT XCO₂. *Environmental Research Letters*, 11(10), 105001. <https://doi.org/10.1088/1748-9326/11/10/105001>
- Ito, A. (2023). Global termite methane emissions have been affected by climate and land-use changes. *Scientific Reports*, 13(1), 17195. <https://doi.org/10.1038/s41598-023-44529-1>
- Ito, A., Patra, P. K., & Umezawa, T. (2023). Bottom-up evaluation of the methane budget in Asia and its subregions. *Global Biogeochemical Cycles*, 37(6), e2023GB007723. <https://doi.org/10.1029/2023GB007723>
- Kondo, M., Ichii, K., Patra, P. K., Canadell, J. G., Poulter, B., Sitch, S., et al. (2018). Land use change and El Niño-Southern Oscillation drive decadal carbon balance shifts in Southeast Asia. *Nature Communications*, 9(1), 1154. <https://doi.org/10.1038/s41467-018-03374-x>
- Kondo, M., Ichii, K., Patra, P. K., Poulter, B., Calle, L., Koven, C., et al. (2018). Plant regrowth as a driver of recent enhancement of terrestrial CO₂ uptake. *Geophysical Research Letters*, 45(10), 4820–4830. <https://doi.org/10.1029/2018GL077633>
- Kondo, M., Patra, P. K., Sitch, S., Friedlingstein, P., Poulter, B., Chevallier, F., et al. (2020). State of the science in reconciling top-down and bottom-up approaches for terrestrial CO₂ budget. *Global Change Biology*, 20(3), 1068–1084. <https://doi.org/10.1111/gcb.14917>
- Kondo, M., Sitch, S., Ciais, P., Achard, F., Kato, E., Pongratz, J., et al. (2022). Are land-use change emissions in Southeast Asia decreasing or increasing? *Global Biogeochemical Cycles*, 36(1), e2020GB006909. <https://doi.org/10.1029/2020GB006909>
- Lauerwald, R., Allen, G., Deemer, B., Liu, S., Maa vara, T., Raymond, P., et al. (2023). Inland water greenhouse gas budgets for RECCAP2: 2 regionalization and homogenization of estimates following the RECCAP2 framework. *Global Biogeochemical Cycles*, 37(5), e2022GB007658. <https://doi.org/10.1029/2022GB007658>
- Li, W., MacBean, N., Ciais, P., Defourny, P., Lamarche, C., Bontemps, S., et al. (2018). Gross and net land cover changes in the main plant functional types derived from the annual ESA CCI land cover maps (1992–2015). *Earth System Science Data*, 10(1), 219–234. <https://doi.org/10.5194/essd-10-219-2018>
- Liu, J., Baskaran, L., Bowman, K., Schimel, D., Bloom, A. A., Parazoo, N. C., et al. (2021). Carbon monitoring system flux net biosphere exchange 2020 (CMS-Flux NBE 2020). *Earth System Science Data*, 13(2), 299–330. <https://doi.org/10.5194/essd-13-299-2021>

- Lohberger, S., Stängel, M., Atwood, E. C., & Siegert, F. (2017). Spatial evaluation of Indonesia's 2015 fire-affected area and estimated carbon emissions using Sentinel-1. *Global Change Biology*, 24(2), 644–654. <https://doi.org/10.1111/gcb.13841>
- Machida, T., Matsueda, H., Sawa, Y., Nakagawa, Y., Hirokuni, K., Kondo, N., et al. (2008). Worldwide measurements of atmospheric CO₂ and other trace gas species using commercial airlines. *Journal of Atmospheric and Oceanic Technology*, 25(10), 1744–1754. <https://doi.org/10.1175/2008JTECHA1082.1>
- Maki, T., Kondo, K., Ishijima, Sekiyama, T. T., Tsuboi, K., & Nakamura, T. (2023). Independent bias correction method for satellite observation data introduced to CO₂ flux inversion. *SOLA*, 19, 157–164. <https://doi.org/10.2151/sola.2023-021>
- Maksyutov, S., Oda, T., Saito, M., Janardanan, R., Belikov, D., Kaiser, J. W., et al. (2021). Technical note: A high-resolution inverse modelling technique for estimating surface CO₂ fluxes based on the NIES-TM-FLEXPART coupled transport model and its adjoint. *Atmospheric Chemistry and Physics*, 21(2), 1245–1266. <https://doi.org/10.5194/acp-21-1245-2021>
- Maksyutov, S., Takagi, H., Valsala, V. K., Saito, M., Oda, T., Saeki, T., et al. (2013). Regional CO₂ flux estimates for 2009–2010 based on GOSAT and ground-based CO₂ observations. *Atmospheric Chemistry and Physics*, 13(18), 9351–9373. <https://doi.org/10.5194/acp-13-9351-2013>
- Matsueda, H., Machida, T., Sawa, Y., Nakagawa, Y., Hirokuni, K., Ikeda, H., et al. (2008). Evaluation of atmospheric CO₂ measurements from new flask air sampling of JAL airliner observations. *Papers in Meteorology and Geophysics*, 59, 1–17. <https://doi.org/10.2467/mripapers.59.1>
- Mayorga, E., Seitzinger, S. P., Harrison, J. A., Dumont, E., Beusen, A. H. W., Bouwman, A. F., et al. (2010). Global nutrient export from WaterSheds 2 (NEWS 2): Model development and implementation. *Environmental Modelling & Software*, 25(7), 837–853. <https://doi.org/10.1016/j.envsoft.2010.01.007>
- McDuffie, E. E., Smith, S. J., O'Rourke, P., Tibrewal, K., Venkataraman, C., Marais, E. A., et al. (2020). A global anthropogenic emission inventory of atmospheric pollutants from sector- and fuel-specific sources (1970–2017): An application of the community emissions data system (CEDS). *Earth System Science Data*, 12(4), 3413–3442. <https://doi.org/10.5194/essd-12-3413-2020>
- McNorton, J., Wilson, C., Gloor, M., Parker, R. J., Boesch, H., Feng, W., et al. (2018). Attribution of recent increases in atmospheric methane through 3-D inverse modelling. *Atmospheric Chemistry and Physics*, 18(24), 18149–18168. <https://doi.org/10.5194/acp-18-18149-2018>
- Melton, J. R., Chan, E., Millard, K., Fortier, M., Winton, R. S., Martín-López, J. M., et al. (2022). A map of global peatland extent created using machine learning (Peat-ML). *Geoscientific Model Development*, 15(12), 4709–4738. <https://doi.org/10.5194/gmd-15-4709-2022>
- Messenger, M. L., Lehner, B., Grill, G., Nedeva, I., & Schmitt, O. (2016). Estimating the volume and age of water stored in global lakes using a geo-statistical approach. *Nature Communications*, 7(1), 13603. <https://doi.org/10.1038/ncomms13603>
- Miettinen, J., Shi, C., & Liew, S. C. (2016). Land-cover distribution in the peatlands of peninsular Malaysia, Sumatra and borneo in 2015 with changes since 1990. *Global Ecology and Conservation*, 6, 67–78. <https://doi.org/10.1016/j.gecco.2016.02.004>
- Mitchard, E. T. A. (2018). The tropical forest carbon cycle and climate change. *Nature*, 559(7715), 527–534. <https://doi.org/10.1038/s41586-018-0300-2>
- Murdiyarso, D., Hergoualc'h, K., & Verchot, L. V. (2010). Opportunities for reducing greenhouse gas emissions in tropical peatlands. *Proceedings of the National Academy of Sciences of the United States of America*, 107(46), 19655–19660. <https://doi.org/10.1073/pnas.0911966107>
- Myers, N., Mittermeier, R. A., Mittermeier, C. G., da Fonseca, G. A. B., & Kent, J. (2000). Biodiversity hotspots for conservation priorities. *Nature*, 403(6772), 853–858. <https://doi.org/10.1038/35002501>
- Niwa, Y., Fujii, Y., Sawa, Y., Iida, Y., Ito, A., Satoh, M., et al. (2017). A 4D-Var inversion system based on the icosahedral grid model (NICAM-TM 4D-Var v1.0) – Part 2: Optimization scheme and identical twin experiment of atmospheric CO₂ inversion. *Geoscientific Model Development*, 10(6), 2201–2219. <https://doi.org/10.5194/gmd-10-2201-2017>
- Niwa, Y., Sawa, Y., Nara, H., Machida, T., Matsueda, H., Umezawa, T., et al. (2021). Estimation of fire-induced carbon emissions from Equatorial Asia in 2015 using in situ aircraft and ship observations. *Atmospheric Chemistry and Physics*, 21(12), 9455–9473. <https://doi.org/10.5194/acp-21-9455-2021>
- Niwa, Y., Tomita, H., Satoh, M., Imasu, R., Sawa, Y., Tsuboi, K., et al. (2017). A 4D-Var inversion system based on the icosahedral grid model (NICAM-TM 4D-Var v1.0) – Part 1: Offline forward and adjoint transport models. *Geoscientific Model Development*, 10(3), 1157–1174. <https://doi.org/10.5194/gmd-10-1157-2017>
- Othman, M., Latif, M. T., Hamid, H. H. A., Uning, R., Khumsaeng, T., Phairuang, W., et al. (2022). Spatial-temporal variability and health impact of particulate matter during a 2019–2020 biomass burning event in Southeast Asia. *Scientific Reports*, 12(1), 7630. <https://doi.org/10.1038/s41598-022-11409-z>
- Page, S. E., & Hooijer, A. (2016). In the line of fire: The peatlands of Southeast Asia. *Philosophical Transactions of the Royal Society B*, 371(1696), 20150176. <https://doi.org/10.1098/rstb.2015.0176>
- Page, S. E., Siegert, F., Rieley, J. O., Boehm, H.-D. V., Jaya, A., & Limin, S. (2002). The amount of carbon released from peat and forest fires in Indonesia during 1997. *Nature*, 420(6911), 61–65. <https://doi.org/10.1038/nature01131>
- Pandey, S., Houweling, S., Krol, M., Aben, I., Chevallier, F., Dlugokencky, E. J., et al. (2016). Inverse modeling of GOSAT-retrieved ratios of total column CH₄ and CO₂ for 2009 and 2010. *Atmospheric Chemistry and Physics*, 16(8), 5043–5062. <https://doi.org/10.5194/acp-16-5043-2016>
- Patra, P. K., Saeki, T., Dlugokencky, E. J., Ishijima, K., Umezawa, T., Ito, A., et al. (2016). Regional methane emission estimation based on observed atmospheric concentrations (2002–2012). *Journal of the Meteorological Society of Japan*, 94(1), 85–107. <https://doi.org/10.2151/jmsj.2016-006>
- Patra, P. K., Takigawa, M., Watanabe, S., Chandra, N., Ishijima, K., & Yamashita, Y. (2018). Improved chemical tracer simulation by MIROC4.0-based atmospheric chemistry-transport model (MIROC4-ACTM). *SOLA*, 14, 91–96. <https://doi.org/10.2151/sola.2018-016>
- Peters, W., Jacobson, A. R., Sweeney, C., Andrews, A. E., Conway, T. J., Masarie, K., et al. (2007). An atmospheric perspective on North American carbon dioxide exchange: Carbon tracker. *Proceedings of the National Academy of Sciences*, 104(48), 18925–18930. <https://doi.org/10.1073/pnas.0708986104>
- Poulter, B., Bastos, A., Canadell, J. G., Ciais, P., Gruber, N., Hauck, J., et al. (2022). Inventorying Earth's land and ocean greenhouse gases. *Eos*, 103. <https://doi.org/10.1029/2022EO179084>
- Pugh, T. A. M., Lindeskog, M., Smith, B., Poulter, B., Arneeth, A., Haverd, V., & Calle, L. (2019). Role of forest regrowth in global carbon sink dynamics. *Proceedings of the National Academy of Sciences of the United States of America*, 116(10), 4382–4387. <https://doi.org/10.1073/pnas.1810512116>
- Qiu, J., Seah, S., & Martinus, M. (2024). Examining climate ambition enhancement in ASEAN countries' nationally determined contributions. *Environmental Development*, 49, 100945. <https://doi.org/10.1016/j.envdev.2023.100945>
- Raymond, P. A., Hartmann, J., Lauerwald, R., Sobek, S., McDonald, C., Hoover, M., et al. (2013). Global carbon dioxide emissions from inland waters. *Nature*, 503, 355–359. <https://doi.org/10.1038/nature13142>

- Richards, D. R., & Friess, D. A. (2015). Rates and drivers of mangrove deforestation in Southeast Asia, 2000–2012. *Proceedings of the National Academy of Sciences of the United States of America*, *113*(2), 344–349. <https://doi.org/10.1073/pnas.1510272113>
- Rosentreter, J. A., Laruelle, G. G., Bange, H. W., Bianchi, T. S., Busecke, J. J. M., Cai, W.-J., et al. (2023). Coastal vegetation and estuaries are collectively a greenhouse gas sink. *Nature Climate Change*, *13*(6), 579–587. <https://doi.org/10.1038/s41558-023-01682-9>
- Saeki, T., & Patra, P. K. (2017). Implications of overestimated anthropogenic CO₂ emissions on East Asian and global land CO₂ flux inversion. *Geoscience Letters*, *4*(1), 9. <https://doi.org/10.1186/s40562-017-0074-7>
- Saunois, M., Stavert, A. R., Poulter, B., Bousquet, P., Canadell, J. G., Jackson, R. B., et al. (2020). The global methane budget 2000–2017. *Earth System Science Data*, *12*(3), 1561–1623. <https://doi.org/10.5194/essd-12-1561-2020>
- Segers, A., & Houweling, S. (2018). Description of the CH₄ inversion production chain, CAMS (copernicus atmospheric monitoring service) report. Retrieved from https://atmosphere.copernicus.eu/sites/default/files/2018-11/CAMS73_2015SSC3_D73.2.5.5-2018_201811_production_chain_v1_0.pdf
- Siegert, F., Ruecker, G., Hinrichs, A., & Hoffmann, A. A. (2001). Increased damage from fires in logged forests during droughts caused by El Niño. *Nature*, *414*(6862), 437–440. <https://doi.org/10.1038/35106547>
- Sodhi, N. S., Koh, L. P., Brook, B. W., & Ng, P. K. L. (2004). Southeast Asian biodiversity: An impending disaster. *Trends in Ecology and Evolution*, *12*(19), 654–660. <https://doi.org/10.1016/j.tree.2004.09.006>
- Sodhi, N. S., Posa, M. R. C., Lee, T. M., Bickford, D., Koh, L. P., & Brook, B. W. (2010). The state and conservation of Southeast Asian biodiversity. *Biodiversity & Conservation*, *19*(2), 317–328. <https://doi.org/10.1007/s10531-009-9607-5>
- Stibig, H.-J., Achard, F., Carboni, S., Raši, R., & Miettinen, J. (2014). Change in tropical forest cover of Southeast Asia from 1990 to 2010. *Biogeosciences*, *11*(2), 247–258. <https://doi.org/10.5194/bg-11-247-2014>
- Tan-Soo, J.-S., & Pattanayak, S. K. (2018). Seeking natural capital projects: Forest fires, haze, and early-life exposure in Indonesia. *Proceedings of the National Academy of Sciences of the United States of America*, *116*(12), 5239–5245. <https://doi.org/10.1073/pnas.1802876116>
- Thirumalai, K., DiNezio, P. N., Okumura, Y., & Deser, C. (2017). Extreme temperatures in Southeast Asia caused by El Niño and worsened by global warming. *Nature Communications*, *8*(1), 15531. <https://doi.org/10.1038/ncomms15531>
- Thompson, R. L., Chevallier, F., Crotwell, A. M., Dutton, G., Langenfelds, R. L., Prinn, R. G., et al. (2014). Nitrous oxide emissions 1999 to 2009 from a global atmospheric inversion. *Atmospheric Chemistry and Physics*, *14*(4), 1801–1817. <https://doi.org/10.5194/acp-14-1801-2014>
- Tian, H., Xu, R., Canadell, J. G., Thompson, R. L., Winiwarter, W., Suntharalingam, P., et al. (2020). A comprehensive quantification of global nitrous oxide sources and sinks. *Nature*, *586*(7828), 248–256. <https://doi.org/10.1038/s41586-020-2780-0>
- Tian, H., Yang, J., Lu, C., Xu, R., Canadell, J. G., Jackson, R. B., et al. (2018). The global N₂O model intercomparison project. *Bulletin of the American Meteorological Society*, *99*(6), 1231–1251. <https://doi.org/10.1175/BAMS-D-17-0212.1>
- Tsuruta, A., Aalto, T., Backman, L., Hakkarainen, J., van der Laan-Luijckx, I. T., Krol, M. C., et al. (2017). Global methane emission estimates for 2000–2012 from Carbon-Tracker Europe-CH₄ v1.0. *Geoscientific Model Development*, *10*(3), 1261–1289. <https://doi.org/10.5194/gmd-10-1261-2017>
- Vadrevu, K. P., Lasko, K., Giglio, L., Schroeder, W., Biswas, S., & Justice, C. (2019). Trends in vegetation fires in South and Southeast Asian countries. *Scientific Reports*, *9*(1), 7422. <https://doi.org/10.1038/s41598-019-43940-x>
- Vancutsem, C., Achard, F., Pekel, J.-F., Vieilledent, G., Carboni, S., Simonetti, D., et al. (2021). Long-term (1990–2019) monitoring of forest cover changes in the humid tropics. *Science Advances*, *7*, 10. <https://doi.org/10.1126/sciadv.abe1603>
- van der Laan-Luijckx, I. T., vander Velde, I. R., van der Veen, E., Tsuruta, A., Stanislawski, K., Babenhausserheide, A., et al. (2017). The CarbonTracker data assimilation shell (CTDAS) v1.0: Implementation and global carbon balance 2001–2015. *Geoscientific Model Development*, *10*(7), 2785–2800. <https://doi.org/10.5194/gmd-10-2785-2017>
- van der Werf, G. R., Dempewolf, J., Trigg, S. N., Randerson, J. T., Kasibhatla, P. S., Giglio, L., et al. (2008). Climate regulation of fire emissions and deforestation in equatorial Asia. *Proceedings of the National Academy of Sciences of the United States of America*, *105*(51), 20350–20355. <https://doi.org/10.1073/pnas.0803375105>
- van der Werf, G. R., Randerson, J. T., Giglio, L., van Leeuwen, T. T., Chen, Y., Rogers, B. M., et al. (2017). Global fire emissions estimates during 1997–2016. *Earth System Science Data*, *9*(2), 697–720. <https://doi.org/10.5194/essd-9-697-2017>
- Wang, F., Maksyutov, S., Tsuruta, A., Janardanan, R., Ito, A., Sasakawa, M., et al. (2019). Methane emission estimates by the global high-resolution inverse model using national inventories. *Remote Sensing*, *11*(21), 2489. <https://doi.org/10.3390/rs11212489>
- Wang, Y., Hollingsworth, P. M., Zhai, D., West, C. D., Green, J. M. H., Chen, H., et al. (2023). High-resolution maps show that rubber causes substantial deforestation. *Nature*, *623*(7986), 340–346. <https://doi.org/10.1038/s41586-023-06642-z>
- Wells, K. C., Millet, D. B., Bousseres, N., Henze, D. K., Chaliyakunnel, S., Griffis, T. J., et al. (2015). Simulation of atmospheric N₂O with GEOS-chem and its adjoint: Evaluation of observational constraints. *Geoscientific Model Development*, *8*(10), 3179–3198. <https://doi.org/10.5194/gmd-8-3179-2015>
- Wetlands International. (2003). Maps of peatland distribution and carbon content in Sumatera (pp. 1990–2002).
- Wetlands International. (2004). Maps of peatland distribution and carbon content in Kalimantan (pp. 2000–2002).
- Wijedasa, L. S., Sloan, S., Page, S. E., Clements, G. R., Lupascu, M., & Evans, T. A. (2018). Carbon emissions from South-East Asian peatlands will increase despite emission-reduction schemes. *Global Change Biology*, *24*(10), 4598–4613. <https://doi.org/10.1111/gcb.14340>
- Wilson, C., Chipperfield, M., Gloor, M., & Chevallier, F. (2014). Development of a variational flux inversion system (INVICAT v1.0) using the TOMCAT chemical transport model. *Geoscientific Model Development*, *7*(5), 2485–2500. <https://doi.org/10.5194/gmd-7-2485-2014>
- Xu, Y., Yu, L., Ciaia, P., Li, W., Santoro, M., Yang, H., & Gong, P. (2022). Recent expansion of oil palm plantations into carbon-rich forests. *Nature Sustainability*, *5*, 574–577. <https://doi.org/10.1038/s41893-022-00897-6>
- Yoshida, Y., Kikuchi, N., Morino, I., Uchino, O., Oshchepkov, S., Bril, A., et al. (2013). Improvement of the retrieval algorithm for GOSAT SWIR XCO₂ and XCH₄ and their validation using TCCON data. *Atmospheric Measurement Techniques*, *6*, 1533–1547. <https://doi.org/10.5194/amt-6-1533-2013>
- Zeng, Z., Estes, L., Ziegler, A. D., Chen, A., Searchinger, T., Hua, F., et al. (2018). Highland cropland expansion and forest loss in Southeast Asia in the twenty-first century. *Nature Geoscience*, *11*(8), 556–562. <https://doi.org/10.1038/s41561-018-0166-9>
- Zheng, B., Chevallier, F., Ciaia, P., Yin, Y., Deeter, M. N., Worden, H. M., et al. (2018). Rapid decline in carbon monoxide emissions and export from East Asia between years 2005 and 2016. *Environmental Research Letters*, *13*(4), 044007. <https://doi.org/10.1088/1748-9326/aab2b3>
- Zheng, B., Chevallier, F., Ciaia, P., Yin, Y., & Wang, Y. (2018). On the role of the flaming to smoldering transition in the seasonal cycle of African fire emissions. *Geophysical Research Letters*, *45*(21), 11998–12007. <https://doi.org/10.1029/2018GL079092>
- Zscheischler, J., Mahecha, M. D., Avitabile, V., Calle, L., Carvalhais, N., Ciaia, P., et al. (2017). Reviews and syntheses: An empirical spatio-temporal description of the global surface–atmosphere carbon fluxes: Opportunities and data limitations. *Biogeosciences*, *14*(15), 3685–3703. <https://doi.org/10.5194/bg-14-3685-2017>